Nonlinear Three-Dimensional Beam Theory for Flexible Multibody Dynamics*

Shilei Han and Olivier A. Bauchau
University of Michigan-Shanghai Jiao Tong University Joint Institute
800 Dong Chuan Road, Shanghai, 200240, China

Abstract

In flexible multibody systems, it is convenient to approximate many structural components as beams or shells. Classical beam theories, such as Euler-Bernoulli beam theory, often form the basis of the analytical development for beam dynamics. The advantage of this approach is that it leads to a very simple kinematic representation of the problem: the beam's section is assumed to remain plane and its displacement field is fully defined by three displacement and three rotation components. While such approach is capable of capturing the kinetic energy of the system accurately, it cannot represent the strain energy adequately. This paper presents a different approach to the problem. Based on a finite element discretization of the cross-section, an exact solution of the theory of three-dimensional elasticity is developed. The proposed approach is based on the Hamiltonian formalism and leads to an expansion of the solution in terms of extremity and central solutions. Kinematically, the problem is decomposed into an arbitrarily large rigid-section motion and a warping field. The sectional strains associated with the rigid-section motion and the warping field are assumed to remain small. As a consequence of this kinematic decomposition, the governing equations of the problem fall into two distinct categories: the equations describing geometrically exact beams and those describing local deformations. The governing equations for geometrically exact beams are nonlinear, one-dimensional equations, whereas a linear, two-dimensional analysis provides the detailed distribution of three-dimensional stress and strain fields. Within the stated assumptions, the solutions presented here are exact solution of three-dimensional elasticity for beams undergoing arbitrarily large motions.

1 Introduction

A beam is defined as a structure having one of its dimensions much larger than the other two. The generally curved axis of the beam is defined along that longer dimension and the cross-section slides along this axis. The cross-section's geometric and physical properties are assumed to vary smoothly along the beam's span. Numerous components found in flexible multibody systems are beam-like structures: linkages, transmission shafts, robotic arms, etc. Aeronautical structures such as aircraft wings or helicopter and wind turbine rotor blades are often treated as beams.

The solid mechanics theory of beams, more commonly referred to simply as "beam theory," plays an important role in structural analysis because it provides designers with simple tools to analyze numerous structures [1]. Several beam theories have been developed based on various assumptions and lead to different levels of accuracy. One of the simplest and most useful of these theories is due to Euler who analyzed the elastic deformation of slender beams. In many applications, beams

Multibody System Dynamics, **34**(3): pp 211-242, 2015

are complex build-up structures with solid or thin-walled cross-sections. Furthermore, laminated composite materials have found increased use in aeronautical constructions leading to heterogeneous, highly anisotropic structures.

The analysis of complex cross-sections featuring composite materials and the determination of the associated sectional properties was first presented by Giavotto *et al.* [2]. Their approach, based on linear elasticity theory, leads to a two-dimensional analysis of the beam's cross-section using finite elements and describes the sectional stiffness characteristics in the form of a 6×6 stiffness matrix relating the six sectional deformations to the corresponding sectional loads. Furthermore, the three-dimensional strain field at all points of the cross-section can be recovered once the sectional strains are known.

While the authors cited above focused on practical applications of engineering beam problems, far more theoretical approaches were developed as well. For instance, Mielke [3, 4] investigated prismatic structures and identified the existence of a "central manifold," equivalent to the "central solutions" presented by Giavotto *et al.* [2]. In a later paper [5], the same author developed a Hamiltonian formulation to the problem.

At the same time, Zhong *et al.* [6, 7, 8] developed novel analytical techniques based on the Hamiltonian formalism for a broad class of linear elasticity problems. A Hamiltonian matrix characterizes the stiffness of the structure and its null eigenvalues give rise to polynomial solutions. Zhong further identified the fact the Hamiltonian matrix cannot be diagonalized, rather, it can be reduced the Jordan canonical form only. Finally, a similar approach was followed by Morandini *et al.* [9] who used numerical techniques to evaluate the Jordan form and associated generalized eigenvectors for cross-sections made of both isotropic and anisotropic materials.

For nonlinear problems, the decomposition of the beam problem into a linear, two-dimensional analysis over the cross-section, and a nonlinear, one-dimensional analysis along its span was first proposed by Berdichevsky [10]. Hodges [11] has reviewed many approaches to beam modeling; he points out that although the two-dimensional finite element analysis of the cross-section seems to be computationally expensive, it is, in fact, a preprocessing step that is performed once only.

Bauchau and Han [12] have formulated beam problems using Hamilton's canonical formulation and have shown that an exact solution of the three-dimensional theory of *static* elasticity can be derived for beams of general cross-sectional shape made of anisotropic materials. This solution provides a sound basis for the more challenging *dynamic* problems found in flexible multibody systems, but an assumption must then be made: the kinetic energy associated with warping is negligible. At high frequencies, *i.e.*, frequencies whose associated wave lengths are comparable to the dimensions of the cross-section or shorter, this assumption is no longer satisfied. Indeed, as frequency increases, local inertial forces, including those due to warping, become increasingly larger. At high frequencies, the beam behaves as a truly three-dimensional structure and should be treated as such, not as a beam. This discussion explains why the kinetic energy of beams is evaluated based on the rigid-section approximation. This practice has been followed by numerous researchers over the last three decades, see, for instance, the work of Simo *et al.* [13], Borri *et al.* [14], Hodges *et al.* [15], or Bauchau *et al.* [16]. The dispersion characteristics of anisotropic beams presenting cross-sections of arbitrary geometry have been studied by Volovoi *et al.* [17]. They concluded that beam theory is inherently a "low frequency approximation" to the three-dimensional theory of elastodynamics.

The present paper generalizes the results of Bauchau and Han [12] to initially curved and twisted beams undergoing arbitrary large displacements and rotations. While still a static analysis only, it provides sound foundations for the dynamic analysis of flexible multibody systems.

2 Kinematics of the problem

Figure 1 depicts an initially curved and twisted beam of length L, with a cross-section of arbitrary shape and area $\mathcal{A}$. The volume of the beam is generated by sliding the cross-section along the reference line of the beam, which is defined by an arbitrary curve in space denoted $\mathcal{C}$. Curvilinear coordinate α_1 defines the intrinsic parameterization of this curve, *i.e.*, it measures length along $\mathcal{C}$. Point **B** is located at the intersection of the reference line with the plane of the cross-section. The unit tangent vector to curve $\mathcal{C}$ is

$$\bar{t} = \frac{\partial \underline{r}_B}{\partial \alpha_1}, \tag{1}$$

where $\underline{r}_B$ is the position vector of point **B** with respect to the origin of the reference frame, $\mathcal{F} = [\mathbf{O}, \mathcal{I} = (\bar{\imath}_1, \bar{\imath}_2, \bar{\imath}_3)]$.

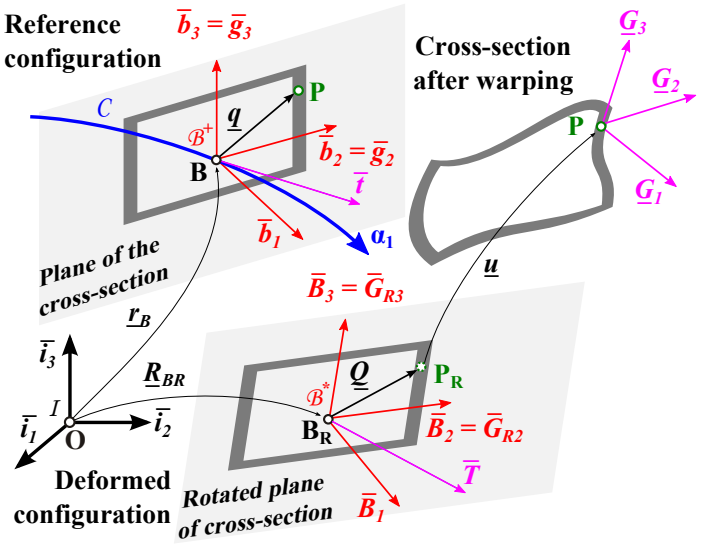

Figure 1: Configuration of a curved beam. To be more illustrative, the figure shows a thin-walled, rectangular cross-section for the beam. For clarity of the figure in the deformed configuration, the cross-section after warping is depicted away from its actual location after the rigid-section motion (In reality, the warping field, $\underline{u}$, is assumed to be small).

In the reference configuration, the cross-section is defined by frame $\mathcal{F}^+ = \left[\mathbf{B}, \mathcal{B}^+ = (\bar{b}_1, \bar{b}_2, \bar{b}_3)\right]$. The plane of the cross-section is determined by two mutually orthogonal unit vectors, $\bar{b}_2$ and $\bar{b}_3$; in general, the unit tangent vector, $\bar{t}$, to curve $\mathcal{C}$ is not aligned with unit vector $\bar{b}_1$, as illustrated in fig. 1. A set of material coordinates that naturally represent the configuration of the beam is selected as follows: α_1, α_2, and α_3, where the last two coordinates measure length along the directions of unit vectors $\bar{b}_2$ and $\bar{b}_3$, respectively.

It is desirable to develop the model using a non-dimensional formulation. A representative dimension of the beam's cross-section, denoted a_r, is used to normalize length, *i.e.*, $\bar{\alpha}_i = \alpha_i / a_r$, $i = 1, 2, 3$, are the non-dimensional coordinates. The orientation of the sectional plane changes as it slides along curve $\mathcal{C}$. Consequently, basis $\mathcal{B}^+$ is a function of curvilinear variable α_1; the rotation tensor that brings basis $\mathcal{I}$ to basis $\mathcal{B}^+$ is denoted $\underline{\underline{R}}_0(\alpha_1)$. The following motion tensor [16] is defined

$$\underline{\underline{\mathcal{C}}}_0(\alpha_1) = \begin{bmatrix} \underline{\underline{R}}_0 & \tilde{r}_B \underline{\underline{R}}_0 \\ \underline{\underline{0}} & \underline{\underline{R}}_0 \end{bmatrix}. \tag{2}$$

The components of the beam's curvature vector in its initial configuration, resolved in basis $\mathcal{B}^+$, are then $\tilde{\bar{k}}_0^+ = \underline{\underline{\mathcal{C}}}_0^{-1} \underline{\underline{\mathcal{C}}}_0'$, where notation $(\cdot)^+$ indicates tensor components resolved in basis $\mathcal{B}^+$ and $(\cdot)'$ a derivative with respect to $\bar{\alpha}_1$. It is verified easily that $\underline{\bar{k}}_0^{+T} = \{\bar{t}^{+T}, \underline{\bar{k}}^{+T}\}$, where $\underline{\bar{k}}^+ = \text{axial}(\underline{\underline{R}}_0^T \underline{\underline{R}}_0')$.

2.1 The reference configuration

With these definitions, the position vector of an arbitrary material point **P** of the beam in its reference configuration becomes

$$\underline{r}_P(\alpha_1,\alpha_2,\alpha_3) = \underline{r}_B(\alpha_1) + \underline{\underline{R}}_0(\alpha_1)\underline{q}^+(\alpha_2,\alpha_3), \tag{3}$$

where vector $\underline{q} = \underline{r}_P - \underline{r}_B$ defines the relative position of point **P** with respect to point **B** and its components resolved in basis $\mathcal{B}^+$ are $\underline{q}^{+T} = \{0, \alpha_2, \alpha_3\}$. The base vectors associated with these material coordinates are

$$\underline{g}_1 = \frac{\partial \underline{r}_P}{\partial \alpha_1} = \underline{\underline{R}}_0 \left(\bar{t}^+ + \tilde{k}^+ \underline{q}^+\right), \tag{4a}$$

$$\underline{g}_2 = \frac{\partial \underline{r}_P}{\partial \alpha_2} = \underline{\underline{R}}_0 \bar{\imath}_2, \tag{4b}$$

$$\underline{g}_3 = \frac{\partial \underline{r}_P}{\partial \alpha_3} = \underline{\underline{R}}_0 \bar{\imath}_3. \tag{4c}$$

The components of these base vectors resolved in basis $\mathcal{B}^+$ are found to be

$$\underline{g}_1^+ = \begin{Bmatrix} \bar{t}_1^+ - \bar{k}_3^+\bar{\alpha}_2 + \bar{k}_2^+\bar{\alpha}_3 \\ \bar{t}_2^+ - \bar{k}_1^+\bar{\alpha}_3 \\ \bar{t}_3^+ + \bar{k}_1^+\bar{\alpha}_2 \end{Bmatrix} = \begin{Bmatrix} \bar{\chi}_1^+ \\ \bar{\chi}_2^+ \\ \bar{\chi}_3^+ \end{Bmatrix}, \quad \underline{g}_2^+ = \begin{Bmatrix} 0 \\ 1 \\ 0 \end{Bmatrix}, \quad \underline{g}_3^+ = \begin{Bmatrix} 0 \\ 0 \\ 1 \end{Bmatrix}. \tag{5}$$

For simplicity, the following notation is introduced, $\bar{\chi}_1^+ = \bar{t}_1^+ - \bar{k}_3^+\bar{\alpha}_2 + \bar{k}_2^+\bar{\alpha}_3$, $\bar{\chi}_2^+ = \bar{t}_2^+ - \bar{k}_1^+\bar{\alpha}_3$, and $\bar{\chi}_3^+ = \bar{t}_3^+ + \bar{k}_1^+\bar{\alpha}_2$. The base vectors in the reference configuration form the tensor defined by eq. (6a); the inverse of this tensor is given by eq. (6b),

$$\underline{\underline{g}}^+ = \left[\bar{t}^+ + \tilde{k}^+\underline{q}^+, \bar{\imath}_2, \bar{\imath}_3\right], \tag{6a}$$

$$\underline{\underline{g}}^{+-1} = \frac{1}{\sqrt{g}} \begin{bmatrix} 1 & 0 & 0 \\ -\bar{\chi}_2^+ & \sqrt{g} & 0 \\ -\bar{\chi}_3^+ & 0 & \sqrt{g} \end{bmatrix}, \tag{6b}$$

where $\sqrt{g} = \bar{\chi}_1^+ = \det(\underline{\underline{g}}^+)$.

2.2 The rigid-section motion

Figure 1 also shows the configuration of the beam in its deformed state. The cross-sectional displacement field is decomposed into two parts: a rigid-section motion and an arbitrary warping field. The "rigid-section motion" of the beam is defined as one which allows arbitrary deformation of its reference line and independent rotation of each cross-section, *i.e.*, each cross-section undergoes a rigid-body motion. This motion is, in fact, the only motion allowed by the Euler-Bernoulli assumptions [1]. After the rigid-section motion, material points **B** and **P** move to points $\mathbf{B_R}$ and $\mathbf{P_R}$, respectively, and the cross-section is defined by frame $\mathcal{F}_R = \left[\mathbf{B_R}, \mathcal{B}^* = (\bar{B}_1, \bar{B}_2, \bar{B}_3)\right]$. The beam's reference line describes a new curve in space denoted $\mathcal{C}_R$.

The rotation of the cross-section is characterized by rotation tensor $\underline{\underline{R}}(\alpha_1)$ that brings basis $\mathcal{B}^+$ to basis $\mathcal{B}^*$ and notation $(\cdot)^*$ indicates tensor components resolved in basis $\mathcal{B}^*$. The following motion tensor is defined

$$\underline{\underline{\mathcal{C}}}_R(\alpha_1) = \begin{bmatrix} (\underline{\underline{R}}\,\underline{\underline{R}}_0) & \tilde{R}_{B_R}(\underline{\underline{R}}\,\underline{\underline{R}}_0) \\ \underline{\underline{0}} & (\underline{\underline{R}}\,\underline{\underline{R}}_0) \end{bmatrix}, \tag{7}$$

where $\underline{R}_{B_R}$ is the position vector of point $\mathbf{B_R}$ with respect to point $\mathbf{O}$. The components of the curvature vector of the beam in its rigid-section configuration, resolved in basis $\mathcal{B}^*$, are then $\tilde{\bar{\mathcal{K}}}^* = \underline{\underline{\mathcal{C}}}_R^{-1}\underline{\underline{\mathcal{C}}}'_R$, where the 6×6 non-dimensional curvature tensor is

$$\tilde{\bar{\mathcal{K}}}^* = \begin{bmatrix} \tilde{\bar{K}}^* & \tilde{\bar{T}}^* \\ \underline{\underline{0}} & \tilde{\bar{K}}^* \end{bmatrix}. \tag{8}$$

It is verified easily that $\bar{\underline{T}}^* = (\underline{\underline{R}}\,\underline{\underline{R}}_0)^T \underline{R}'_{B_R}$ are the components of the vector tangent to curve $\mathcal{C}_R$ and $\bar{\underline{K}}^* = \text{axial}[(\underline{\underline{R}}\,\underline{\underline{R}}_0)^T(\underline{\underline{R}}\,\underline{\underline{R}}_0)']$. By analogy, the components of the virtual motion vector, $\underline{\delta\mathcal{U}}^*_R$, resolved in basis $\mathcal{B}^*$, are defined as $\underline{\delta\mathcal{U}}^*_R = \mathcal{A}\text{xial}(\underline{\underline{\mathcal{C}}}_R^{-1}\delta\underline{\underline{\mathcal{C}}}_R)$.

In the rigid-section motion configuration, the position vector of a material point becomes

$$\underline{R}_{P_R}(\alpha_1, \alpha_2, \alpha_3) = \underline{R}_{B_R} + (\underline{\underline{R}}\,\underline{\underline{R}}_0)\underline{Q}^*, \tag{9}$$

where $\underline{Q} = \underline{R}_{B_R} - \underline{R}_{P_R}$ denotes the position vector of point $\mathbf{P_R}$ with respect to point $\mathbf{B_R}$. Given the kinematic description of the problem, $\underline{Q}^{*T} = \underline{q}^{+T} = \{0, \alpha_2, \alpha_3\}$. The base vectors in the rigid-section configuration, defined as $\underline{G}_{Ri} = \partial \underline{R}_{P_R}/\partial\alpha_i$, $i = 1, 2, 3$, are now obtained easily as

$$\underline{G}_{R1} = (\underline{\underline{R}}\,\underline{\underline{R}}_0)\left(\bar{\underline{T}}^* + \tilde{\bar{K}}^*\underline{\bar{Q}}^*\right), \tag{10a}$$

$$\underline{G}_{R2} = (\underline{\underline{R}}\,\underline{\underline{R}}_0)\bar{\imath}_2, \tag{10b}$$

$$\underline{G}_{R3} = (\underline{\underline{R}}\,\underline{\underline{R}}_0)\bar{\imath}_3. \tag{10c}$$

The components of the base vectors resolved in basis $\mathcal{B}^*$ are simply $\underline{G}^*_{Ri} = (\underline{\underline{R}}\,\underline{\underline{R}}_0)^T\underline{G}_{Ri}$, $i = 1, 2, 3$, and can be recast in a compact form as $\underline{\underline{G}}^*_R = [\underline{G}^*_{R1}, \underline{G}^*_{R2}, \underline{G}^*_{R3}]$. The expressions of $\underline{\underline{G}}^*_R$ and its inverse are found as

$$\underline{\underline{G}}^*_R = \left[\bar{\underline{T}}^* + \tilde{\bar{K}}^*\bar{\underline{Q}}^*, \bar{\imath}_2, \bar{\imath}_3\right], \tag{11a}$$

$$\underline{\underline{G}}^{*-1}_R = \frac{1}{\sqrt{G}}\begin{bmatrix} 1 & 0 & 0 \\ -\bar{\chi}^*_2 & \sqrt{G} & 0 \\ -\bar{\chi}^*_3 & 0 & \sqrt{G} \end{bmatrix}, \tag{11b}$$

where $\sqrt{G} = \bar{\chi}^*_1 = \det(\underline{\underline{G}}^*_R)$, and for simplicity, the following notation is introduced, $\bar{\chi}^*_1 = \bar{T}^*_1 - \bar{K}^*_3\bar{\alpha}_2 + \bar{K}^*_2\bar{\alpha}_3$, $\bar{\chi}^*_2 = \bar{T}^*_2 - \bar{K}^*_1\bar{\alpha}_3$, and $\bar{\chi}^*_3 = \bar{T}^*_3 + \bar{K}^*_1\bar{\alpha}_2$.

2.3 The deformed configuration

The cross-sectional displacement field was decomposed into two parts: the rigid-section motion discussed in the previous section and an arbitrary warping field, denoted $\underline{u}(\alpha_1, \alpha_2, \alpha_3)$, which describes the relative displacement of material point $\mathbf{P}$ with respect to point $\mathbf{P_R}$. Because the warping field is arbitrary, it includes a rigid-body motion, and hence, rigid-body motions are double counted. This ambiguity will be resolved by the solution process, which determines both rigid-body motions unambiguously, see eq. (71a). In the deformed configuration, the position vector of a material point becomes

$$\underline{R}_P(\alpha_1, \alpha_2, \alpha_3) = \underline{R}_{P_R}(\alpha_1, \alpha_2, \alpha_3) + \underline{u} = \underline{R}_{P_R} + (\underline{\underline{R}}\,\underline{\underline{R}}_0)\underline{u}^*. \tag{12}$$

The base vectors in the deformed configuration, defined as $\underline{G}_i = \partial\underline{R}_P/\partial\alpha_i$, $i = 1, 2, 3$, now

become

$$\underline{G}_1 = \underline{G}_{R1} + (\underline{\underline{R}}\,\underline{\underline{R}}_0)(\tilde{\bar{\underline{K}}}^*\underline{\bar{u}}^* + \frac{\partial \underline{\bar{u}}^*}{\partial \bar{\alpha}_1}), \tag{13a}$$

$$\underline{G}_2 = \underline{G}_{R2} + (\underline{\underline{R}}\,\underline{\underline{R}}_0)\frac{\partial \underline{\bar{u}}^*}{\partial \bar{\alpha}_2}, \tag{13b}$$

$$\underline{G}_3 = \underline{G}_{R3} + (\underline{\underline{R}}\,\underline{\underline{R}}_0)\frac{\partial \underline{\bar{u}}^*}{\partial \bar{\alpha}_3}, \tag{13c}$$

where $\underline{\bar{u}}^* = \underline{u}^*/a_r$ are the non-dimensional components of the warping field resolved in basis $\mathcal{B}^*$.

The components of the base vectors resolved in basis $\mathcal{B}^*$ are simply $\underline{G}_i^* = (\underline{\underline{R}}\,\underline{\underline{R}}_0)^T\underline{G}_i$, $i = 1, 2, 3$, and they can be rewritten in a compact form as $\underline{\underline{G}}^* = [\underline{G}_1^*, \underline{G}_2^*, \underline{G}_3^*]$, which are found as

$$\underline{\underline{G}}^* = \underline{\underline{G}}_R^* + \left[\tilde{\bar{\underline{K}}}^*\underline{\bar{u}}^* + \frac{\partial \underline{\bar{u}}^*}{\partial \bar{\alpha}_1}, \frac{\partial \underline{\bar{u}}^*}{\partial \bar{\alpha}_2}, \frac{\partial \underline{\bar{u}}^*}{\partial \bar{\alpha}_3}\right]. \tag{14}$$

2.4 The strain components

The components of deformation gradient tensor in the mixed bases $\mathcal{B}^*$ and $\mathcal{B}^+$ is defined as

$$\underline{\underline{F}}^{*+} = \underline{\underline{G}}^*\underline{g}^{+-1} = (\underline{\underline{G}}^*\underline{\underline{G}}_R^{*-1})(\underline{\underline{G}}_R^*\underline{g}^{+-1}) = \underline{\underline{F}}_W\underline{\underline{F}}_R, \tag{15}$$

where the second equality corresponds to a multiplicative decomposition of the deformation gradient tensor into its components due to the rigid-section motion, $\underline{\underline{F}}_R$, and warping deformation, $\underline{\underline{F}}_W$.

With the help of eqs. (11a) and (6b), the rigid-section motion component becomes

$$\underline{\underline{F}}_R = \underline{\underline{I}} + \left[\frac{1}{\sqrt{g}}(\underline{\epsilon}^* + \tilde{\bar{Q}}^{*T}\underline{\varkappa}^*), \underline{0}, \underline{0}\right] = \underline{\underline{I}} + \underline{\underline{E}}_R^*, \tag{16}$$

where $\underline{\underline{I}}$ denotes the identity matrix and the sectional strain components associated with the rigid-section motion are defined as

$$\underline{\bar{\mathcal{E}}}_R^* = \underline{\bar{\mathcal{K}}}^* - \underline{\bar{k}}_0^+ = \begin{Bmatrix} \underline{\epsilon}^* \\ \underline{\bar{\varkappa}}^* \end{Bmatrix} = \begin{Bmatrix} (\underline{\underline{R}}\,\underline{\underline{R}}_0)^T\underline{\bar{R}}'_{B_R} - \bar{t}^+ \\ \underline{\underline{R}}_0^T\text{axial}(\underline{\underline{R}}^T\underline{\underline{R}}') \end{Bmatrix}. \tag{17}$$

The strain components, denoted $\underline{\epsilon}^*$, are related to the derivative of the rigid-section displacement of material point **B**. The curvature components, denoted $\underline{\bar{\varkappa}}^*$, are related to the derivatives of cross-sectional rotations. Next, the explicit expression for the warping related component of the deformation gradient tensor is obtained by using eqs. (14) and (11b),

$$\underline{\underline{F}}_W = \underline{\underline{I}} + \left[\frac{1}{\sqrt{G}}(\tilde{\bar{\underline{K}}}^*\underline{\bar{u}}^* + \frac{\partial \underline{\bar{u}}^*}{\partial \bar{\alpha}_1} - \bar{\chi}_2^*\frac{\partial \underline{\bar{u}}^*}{\partial \bar{\alpha}_2} - \bar{\chi}_3^*\frac{\partial \underline{\bar{u}}^*}{\partial \bar{\alpha}_3}), \frac{\partial \underline{\bar{u}}^*}{\partial \bar{\alpha}_2}, \frac{\partial \underline{\bar{u}}^*}{\partial \bar{\alpha}_3}\right] = \underline{\underline{I}} + \underline{\underline{E}}_W^*. \tag{18}$$

It is now assumed that the beam undergoes an arbitrarily large motion while the sectional strains associated with rigid-section motion and warping displacement components remain very small at all times, implying $\|\underline{\underline{E}}_R^*\| \ll 1$ and $\|\underline{\underline{E}}_W^*\| \ll 1$. The deformation gradient tensor then becomes $\underline{\underline{F}}^{*+} \approx \underline{\underline{I}} + (\underline{\underline{E}}_R^* + \underline{\underline{E}}_W^*)$ and the Green-Lagrange strain tensor, defined as $\underline{\underline{e}}^* = (\underline{\underline{F}}^{*+T}\underline{\underline{F}}^{*+} - \underline{\underline{I}})/2$, reduces to

$$\underline{\underline{e}}^* \approx \underline{\underline{\gamma}}^* = \frac{(\underline{\underline{E}}_R^* + \underline{\underline{E}}_W^*) + (\underline{\underline{E}}_R^* + \underline{\underline{E}}_W^*)^T}{2}. \tag{19}$$

Clearly, the small strain assumption implies that the multiplicative decomposition of the deformation gradient tensor expressed by eq. (15) results in an additive decomposition of the corresponding strain tensors.

The components of the strain tensor are partitioned into the out-of-plane and in-plane strain components, denoted $\underline{\gamma}_O^{*T} = \{\gamma_{11}^*, 2\gamma_{12}^*, 2\gamma_{13}^*\}$ and $\underline{\gamma}_I^{*T} = \{\gamma_{22}^*, \gamma_{33}^*, 2\gamma_{23}^*\}$, respectively. Using eqs. (16) and (18) yields

$$\sqrt{g}\,\underline{\gamma}_O^* = \underline{\bar{u}}^{*\prime} + \underline{\underline{\bar{D}}}_O \underline{\bar{u}}^* + (\underline{\epsilon}^* - \tilde{\bar{q}}^+ \underline{\bar{\varkappa}}^*), \tag{20a}$$

$$\sqrt{g}\,\underline{\gamma}_I^* = \underline{\underline{\bar{D}}}_I \underline{\bar{u}}^*. \tag{20b}$$

The following differential operators were defined

$$\underline{\underline{\bar{D}}}_O = \begin{bmatrix} \bar{d} & -\bar{k}_3^+ & \bar{k}_2^+ \\ \bar{k}_3^+ + \sqrt{g}\dfrac{\partial}{\partial\bar{\alpha}_2} & \bar{d} & -\bar{k}_1^+ \\ -\bar{k}_2^+ + \sqrt{g}\dfrac{\partial}{\partial\bar{\alpha}_3} & \bar{k}_1^+ & \bar{d} \end{bmatrix}, \; \underline{\underline{\bar{D}}}_I = \begin{bmatrix} 0 & \sqrt{g}\dfrac{\partial}{\partial\bar{\alpha}_2} & 0 \\ 0 & 0 & \sqrt{g}\dfrac{\partial}{\partial\bar{\alpha}_3} \\ 0 & \sqrt{g}\dfrac{\partial}{\partial\alpha_3} & \sqrt{g}\dfrac{\partial}{\partial\bar{\alpha}_2} \end{bmatrix}, \tag{21}$$

where $\bar{d} = -\bar{\chi}_2^+ \partial(\cdot)/\partial\bar{\alpha}_2 - \bar{\chi}_3^+ \partial(\cdot)/\partial\bar{\alpha}_3$.

The strain components are collected into a single array,

$$\underline{\gamma}^* = \begin{Bmatrix} \underline{\gamma}_O^* \\ \underline{\gamma}_I^* \end{Bmatrix} = \underline{\underline{\bar{A}}}\,\underline{\bar{u}}^{*\prime} + \underline{\underline{\bar{B}}}\,\underline{\bar{u}}^* + \underline{\underline{\bar{\Gamma}}}\,\underline{\bar{\mathcal{E}}}_R^*, \tag{22}$$

where the first two terms describe the strain distribution associated with the warping field and the last term gives the additional strain distribution stemming from the derivative of the rigid-section motion. The following differential operators were defined

$$\underline{\underline{\bar{A}}} = \frac{1}{\sqrt{g}} \begin{bmatrix} \underline{\underline{I}} \\ \underline{\underline{0}} \end{bmatrix}, \quad \underline{\underline{\bar{B}}} = \frac{1}{\sqrt{g}} \begin{bmatrix} \underline{\underline{\bar{D}}}_O \\ \underline{\underline{\bar{D}}}_I \end{bmatrix}, \quad \underline{\underline{\bar{\Gamma}}} = \frac{1}{\sqrt{g}} \begin{bmatrix} \underline{\underline{I}} & \tilde{\bar{q}}^{+T} \\ \underline{\underline{0}} & \underline{\underline{0}} \end{bmatrix}. \tag{23}$$

Because the sectional strains associated with the rigid-section motion are small, eq. (17) implies $\underline{\bar{T}}^* \approx \bar{t}^+$ and $\underline{\bar{K}}^* \approx \underline{\bar{k}}^+$, leading to $\bar{\chi}_i^* \approx \bar{\chi}_i^+$, $i = 1, 2, 3$, and hence, $\sqrt{G} \approx \sqrt{g}$. These consequences of the small strain approximation are reflected in eqs. (20) to (23).

The following transpositional relationships [16] are obtained easily

$$\delta\underline{\bar{\mathcal{E}}}_R^* = \underline{\delta\mathcal{U}}_R^{*\prime} + \tilde{\bar{\mathcal{K}}}^* \underline{\delta\mathcal{U}}_R^*. \tag{24}$$

2.5 Semi-discretization of the warping field

The following semi-discretization of the warping field, first proposed by Giavotto *et al.* [2], is performed

$$\underline{\bar{u}}^*(\bar{\alpha}_1, \bar{\alpha}_2, \bar{\alpha}_3) = \underline{\underline{N}}(\bar{\alpha}_2, \bar{\alpha}_3)\underline{\hat{u}}(\bar{\alpha}_1), \tag{25}$$

where matrix $\underline{\underline{N}}(\bar{\alpha}_2, \bar{\alpha}_3)$ stores the two-dimensional shape functions used in the discretization and array $\underline{\hat{u}}(\bar{\alpha}_1)$ the nodal values of the non-dimensional warping field. Notation $\hat{(\cdot)}$ indicates nodal quantities of the discretized model. The semi-discretization procedure leads to a numerical treatment of the solution for variables $\bar{\alpha}_2$ and $\bar{\alpha}_3$ whereas the dependency of the solution on variable $\bar{\alpha}_1$ is treated analytically.

It will also be required to discretize operator $\underline{\underline{\bar{\Gamma}}}$ defined by eq. (23). The following result is found easily

$$\underline{\underline{\bar{\Gamma}}} = \underline{\underline{\bar{A}}} \begin{bmatrix} 1 & 0 & 0 & 0 & \bar{\alpha}_3 & -\bar{\alpha}_2 \\ 0 & 1 & 0 & -\bar{\alpha}_3 & 0 & 0 \\ 0 & 0 & 1 & \bar{\alpha}_2 & 0 & 0 \end{bmatrix} = \underline{\underline{\bar{A}}}\,\underline{\bar{z}} = \underline{\underline{\bar{A}}}\,\underline{\underline{N}}\,\underline{\underline{\bar{Z}}}, \tag{26}$$

where matrix $\underline{\underline{\bar{Z}}}$ stacks the rows of matrix $\underline{\underline{\bar{z}}}$ for each of the nodes of the model. It now becomes possible to express the components of Green-Lagrange's strain tensor defined by eq. (22) in terms of the nodal displacements as

$$\underline{\gamma}^* = \underline{\underline{\bar{A}}}\,\underline{\underline{N}}\left(\underline{\hat{u}}' + \underline{\underline{\bar{Z}}}\,\underline{\bar{\mathcal{E}}}_R^*\right) + \underline{\underline{\bar{B}}}\,\underline{\underline{N}}\,\underline{\hat{u}}. \tag{27}$$

3 Governing equations

Because much of the work presented here relies on Hamilton's formulation, the beam's governing equations will be derived using Hamilton's canonical approach. The more classical method based on the principle of virtual work could be used as well and leads to identical results. For small strain problems, the components of Green-Lagrange's strain tensor, $\underline{\gamma}^*$, are energetically conjugated to the components of the convected Cauchy stress tensor, denoted $\underline{\tau}^*$, over the reference configuration of the structure, leading to the expression for the strain energy.

3.1 Strain energy expression

The strain energy stored in a slice of the beam of infinitesimal span $\mathrm{d}\alpha_1$ is

$$L = \frac{1}{2}\int_v \underline{\gamma}^{*T}\underline{\tau}^*\ \mathrm{d}v = \frac{1}{2}\int_{\mathcal{A}} \underline{\gamma}^{*T}\underline{\underline{\mathcal{D}}}^*\,\underline{\gamma}^*\ \sqrt{g}\mathrm{d}\mathcal{A}\mathrm{d}\alpha_1, \tag{28}$$

where v is the volume of the slice in the beam's reference configuration. In the second equality, the components of the convected Cauchy stress tensor are related to the Green-Lagrange strain components using constitutive laws for linearly elastic materials

$$\underline{\tau}^* = \underline{\underline{\mathcal{D}}}^*\underline{\gamma}^*, \tag{29}$$

where $\underline{\underline{\mathcal{D}}}^*$ is a 6×6 stiffness matrix for the material, resolved in material basis $\mathcal{B}^*$. The non-dimensional form of the constitutive laws is $\bar{\underline{\tau}}^* = \underline{\underline{\bar{\mathcal{D}}}}^*\underline{\gamma}^*$, where $\bar{\underline{\tau}}^* = \underline{\tau}^*/E_r$, $\underline{\underline{\bar{\mathcal{D}}}}^* = \underline{\underline{\mathcal{D}}}^*/E_r$, and E_r is a representative value of Young's modulus. In the present formulation, the strain energy of the system is the Lagrangian of the problem. As was done for the components of the Green-Lagrange strain tensor, the components of the convected Cauchy stress tensor are partitioned into out-of-plane and in-plane components, denoted $\underline{\tau}_O^*$ and $\underline{\tau}_I^*$, respectively, *i.e.*, $\underline{\tau}^{*T} = [\underline{\tau}_O^{*T}, \underline{\tau}_I^{*T}]$.

Introducing the discretized components of Green-Lagrange's strain tensor given by eq. (27), the strain energy becomes

$$2\bar{L} = \left(\underline{\hat{u}}' + \underline{\underline{\bar{Z}}}\,\underline{\mathcal{E}}_R^*\right)^T\left[\underline{\underline{\bar{M}}}\left(\underline{\hat{u}}' + \underline{\underline{\bar{Z}}}\,\underline{\mathcal{E}}_R^*\right) + \underline{\underline{\bar{C}}}^T\underline{\hat{u}}\right] + \underline{\hat{u}}^T\left[\underline{\underline{\bar{C}}}\left(\underline{\hat{u}}' + \underline{\underline{\bar{Z}}}\,\underline{\mathcal{E}}_R^*\right) + \underline{\underline{\bar{E}}}\,\underline{\hat{u}}\right], \tag{30}$$

where $\bar{L} = L/(a_r^2 E_r)$ is the non-dimensional strain energy and matrices $\underline{\underline{\bar{M}}}$, $\underline{\underline{\bar{C}}}$, and $\underline{\underline{\bar{E}}}$ are defined as

$$\underline{\underline{\bar{M}}} = \int_{\bar{\mathcal{A}}} (\underline{\underline{\bar{A}}}\,\underline{\underline{N}})^T\underline{\underline{\bar{\mathcal{D}}}}^*(\underline{\underline{\bar{A}}}\,\underline{\underline{N}})\ \sqrt{g}\mathrm{d}\bar{\mathcal{A}}, \tag{31a}$$

$$\underline{\underline{\bar{C}}} = \int_{\bar{\mathcal{A}}} (\underline{\underline{\bar{B}}}\,\underline{\underline{N}})^T\underline{\underline{\bar{\mathcal{D}}}}^*(\underline{\underline{\bar{A}}}\,\underline{\underline{N}})\ \sqrt{g}\mathrm{d}\bar{\mathcal{A}}, \tag{31b}$$

$$\underline{\underline{\bar{E}}} = \int_{\bar{\mathcal{A}}} (\underline{\underline{\bar{B}}}\,\underline{\underline{N}})^T\underline{\underline{\bar{\mathcal{D}}}}^*(\underline{\underline{\bar{B}}}\,\underline{\underline{N}})\ \sqrt{g}\mathrm{d}\bar{\mathcal{A}}, \tag{31c}$$

where $\bar{\mathcal{A}} = \mathcal{A}/a_r^2$ is the non-dimensional area of the cross-section. Assuming that the beam's cross-section has been discretized using N nodes, the total number of degrees of freedom is $n = 3N$ and matrices $\underline{\underline{\bar{M}}}$, $\underline{\underline{\bar{C}}}$, and $\underline{\underline{\bar{E}}}$ are of size $n\times n$.

Following the development of Hamilton's canonical formulation, a set of dual variables, denoted $\underline{\hat{P}}$, is introduced

$$\underline{\hat{P}} = \frac{\partial \bar{L}}{\partial \left(\underline{\hat{u}}' + \underline{\underline{\bar{Z}}}\,\underline{\mathcal{E}}_R^*\right)} = \underline{\underline{\bar{M}}}\left(\underline{\hat{u}}' + \underline{\underline{\bar{Z}}}\,\underline{\mathcal{E}}_R^*\right) + \underline{\underline{\bar{C}}}^T\,\underline{\hat{u}}. \tag{32}$$

Introducing eq. (31a) and (31b) into eq. (32) and using expression (27) for the discretized Green-Lagrange strains, the explicit expression of the dual variables is found,

$$\underline{\hat{P}} = \int_{\bar{\mathcal{A}}} \underline{\underline{N}}^T \underline{\mathcal{T}}_O^*\, \mathrm{d}\bar{\mathcal{A}}. \tag{33}$$

The dual variables represent the nodal stress vectors acting on the beam's cross-section. This simple interpretation justifies the selection of the dual variables defined by eq. (32).

Next, the non-dimensional Hamiltonian of the system, denoted $\bar{H}$, is defined via Legendre's transformation [18] as $\bar{H} = \underline{\hat{P}}^T\left(\underline{\hat{u}}' + \underline{\underline{\bar{Z}}}\,\underline{\mathcal{E}}_R^*\right) - \bar{L}$ and tedious algebra reveals that $\bar{H} = 1/2\ \underline{\hat{\mathcal{X}}}^T\,\underline{\underline{\bar{\mathcal{F}}}}\,\underline{\hat{\mathcal{X}}}$, where array $\underline{\hat{\mathcal{X}}}$ stores the nodal warping and forces

$$\underline{\hat{\mathcal{X}}} = \begin{Bmatrix} \underline{\hat{u}} \\ \underline{\hat{P}} \end{Bmatrix}, \tag{34}$$

and matrix $\underline{\underline{\bar{\mathcal{F}}}}$ is defined as

$$\underline{\underline{\bar{\mathcal{F}}}} = \begin{bmatrix} \underline{\underline{\bar{C}}}\,\underline{\underline{\bar{M}}}^{-1}\underline{\underline{\bar{C}}}^T - \underline{\underline{\bar{E}}} & -\underline{\underline{\bar{C}}}\,\underline{\underline{\bar{M}}}^{-1} \\ -(\underline{\underline{\bar{C}}}\,\underline{\underline{\bar{M}}}^{-1})^T & \underline{\underline{\bar{M}}}^{-1} \end{bmatrix}. \tag{35}$$

Hamilton's canonical approach provides two sets of equations. The first set, $\underline{\hat{u}}' + \underline{\underline{\bar{Z}}}\,\underline{\mathcal{E}}_R^* = \partial\bar{H}/\partial\underline{\hat{P}}$, is identical to eqs. (32), *i.e.*, merely defines the nodal forces. The second set, $\underline{\hat{P}}' = -\partial\bar{H}/\partial\underline{\hat{u}}$, provides the governing equations of the problem. The combination of the two sets defines $2n$ first-order, ordinary differential equations with constant coefficients

$$\underline{\hat{\mathcal{X}}}' = \underline{\underline{\bar{\mathcal{H}}}}\,\underline{\hat{\mathcal{X}}} - \underline{\underline{\mathcal{Z}}}\,\bar{\mathcal{E}}_R^*, \tag{36}$$

where matrix $\underline{\underline{\bar{\mathcal{H}}}}$, of size $2n \times 2n$, is defined as

$$\underline{\underline{\bar{\mathcal{H}}}} = \begin{bmatrix} -\underline{\underline{\bar{M}}}^{-1}\underline{\underline{\bar{C}}}^T & \underline{\underline{\bar{M}}}^{-1} \\ \underline{\bar{E}} - \underline{\underline{\bar{C}}}\,\underline{\underline{\bar{M}}}^{-1}\underline{\underline{\bar{C}}}^T & \underline{\underline{\bar{C}}}\,\underline{\underline{\bar{M}}}^{-1} \end{bmatrix} = \underline{\underline{\mathcal{J}}}\,\underline{\underline{\bar{\mathcal{F}}}}, \tag{37}$$

and matrix $\underline{\underline{\mathcal{Z}}}$, of size $2n \times 6$, as

$$\underline{\underline{\mathcal{Z}}} = \begin{bmatrix} \underline{\underline{\bar{Z}}} \\ \underline{\underline{0}} \end{bmatrix}. \tag{38}$$

In view of definition (73), it is verified easily that matrix $\underline{\underline{\bar{\mathcal{H}}}}$ is Hamiltonian and matrix $\underline{\underline{\mathcal{J}}}$ is defined by eq. (74).

The fundamental equation of this work, eq. (36), combines two types of unknowns. First, array $\underline{\hat{\mathcal{X}}}$ stores the nodal warping field, $\underline{\hat{u}}$, that describes the local, three-dimensional deformation of the beam and the associated nodal forces, $\underline{\hat{P}}$, acting on the beam's cross-section. Second, array $\bar{\mathcal{E}}_R^*$ stores the sectional strains associated with the rigid-section motion. Classical beam theories, such as Euler-Bernoulli beam theory, assume that beam deformations are described by rigid-section motion only. Equation (36), which stems from three-dimensional elasticity directly, underlines the shortcomings of such assumptions: rigid-section motion and local three-dimensional deformations are coupled inherently. The rigid-section motions of classical beam theories cannot be obtained without solving the underlying three-dimensional elasticity problem.

3.2 Rigid-body motions

Section 2 has described the decomposition of the displacement field into a rigid-section motion and a warping field; both fields generate local strains. In contrast, this section examines a true rigid-body motion of the beam, *i.e.*, a motion for which all strains vanish. Consider a rigid-body displacement field written as $\underline{u} = \underline{u}_R - \tilde{q}\underline{\phi}_R$, where $\underline{u}_R$ are the components of a rigid-body translation and $\underline{\phi}_R$ those of an infinitesimal rigid-body rotation. For convenience, the following non-dimensional rigid-body motion array is defined $\bar{\underline{\mathcal{U}}}_R^T = \{\bar{\underline{u}}_R^T, \underline{\phi}_R^T\}$ and the nodal displacements become $\hat{\underline{u}} = \bar{\underline{\underline{Z}}}\,\bar{\underline{\mathcal{U}}}_R^*$, where $\bar{\underline{\mathcal{U}}}_R^* = \underline{\underline{\mathcal{C}}}_R^{-1}\bar{\underline{\mathcal{U}}}_R$ is the corresponding rigid-body motion array resolved in basis $\mathcal{B}^*$. Because array $\bar{\underline{\mathcal{U}}}_R$ represents a rigid-body motion, its spatial derivative vanishes, $\bar{\underline{\mathcal{U}}}_R' = \underline{0}$, and hence, $\underline{\mathcal{U}}_R^{*\prime} = -\tilde{\bar{\mathcal{K}}}^*\underline{\mathcal{U}}_R^*$, leading to $\hat{\underline{u}}' = -\bar{\underline{\underline{Z}}}\,\tilde{\bar{\mathcal{K}}}^*\bar{\underline{\mathcal{U}}}_R^*$.

For this rigid-body motion, the nodal forces vanish and eqs. (36) yield $\underline{\underline{\bar{M}}}\,\hat{\underline{u}}' + \underline{\underline{\bar{C}}}^T\hat{\underline{u}} = \underline{0}$ and $\underline{\underline{\bar{E}}}\,\hat{\underline{u}} + \underline{\underline{\bar{C}}}\,\hat{\underline{u}}' = \underline{0}$ or $(\underline{\underline{\bar{C}}}^T\underline{\underline{\bar{Z}}} - \underline{\underline{\bar{M}}}\,\underline{\underline{\bar{Z}}}\,\tilde{\bar{\mathcal{K}}}^*)\bar{\underline{\mathcal{U}}}_R^* = \underline{0}$ and $(\underline{\underline{\bar{E}}}\,\underline{\underline{\bar{Z}}} - \underline{\underline{\bar{C}}}\,\underline{\underline{\bar{Z}}}\,\tilde{\bar{\mathcal{K}}}^*)\bar{\underline{\mathcal{U}}}_R^* = \underline{0}$. Because the rigid-body motion is arbitrary, the following matrix identities result,

$$\underline{\underline{\bar{C}}}^T\underline{\underline{\bar{Z}}} = \underline{\underline{\bar{M}}}\,\underline{\underline{\bar{Z}}}\,\tilde{\bar{\mathcal{K}}}^*, \tag{39a}$$

$$\underline{\underline{\bar{E}}}\,\underline{\underline{\bar{Z}}} = \underline{\underline{\bar{C}}}\,\underline{\underline{\bar{Z}}}\,\tilde{\bar{\mathcal{K}}}^*. \tag{39b}$$

3.3 Stress resultants

Matrix $\bar{\underline{\underline{Z}}}$ also plays an important role in the evaluation of the sectional stress resultants. The first three components of array $\bar{\underline{\underline{Z}}}^T\hat{\underline{P}}$ corresponds to the summation of the nodal forces over the beam's cross-section, and the last three components correspond to the sums of the moments of the same forces, leading to

$$\bar{\underline{\mathcal{F}}}^* = \left\{\begin{array}{c}\bar{\underline{f}}^* \\ \bar{\underline{m}}^*\end{array}\right\} = \bar{\underline{\underline{Z}}}^T\hat{\underline{P}}. \tag{40}$$

where $\bar{\underline{f}}^{*T} = \left\{\bar{N}_1^*, \bar{N}_2^*, \bar{N}_3^*\right\}$ and $\bar{\underline{m}}^{*T} = \left\{\bar{M}_1^*, \bar{M}_2^*, \bar{M}_3^*\right\}$ are the components of the non-dimensional stress resultant forces and moments, respectively, resolved in basis $\mathcal{B}^*$. The sectional forces include the axial force, N_1^*, and the two transverse shear forces, N_2^* and N_3^*, the moments include the twisting moment, M_1^*, and the two bending moments, M_2^* and M_3^*.

3.4 Characteristics of the governing equations

Bauchau and Han [12] have discussed the characteristics of the governing equations and their impact on the nature of the solution. Because the governing equations (36) are first-order, ordinary differential equations with constant coefficients, the nature of their solutions depends on the eigenvalues of the system matrix, Hamiltonian matrix $\underline{\underline{\mathcal{H}}}$. An arbitrary stress distribution applied over the cross-section can be decomposed unequivocally into six stress resultants and a self-equilibrating stress distribution. The six stress resultants excite the central solutions, which are associated with polynomial solutions that propagate over the beam's entire span. On the other hand, the self-equilibrating stress distribution excite the extremity solutions, which are solutions decaying exponentially away from the beam's edges.

The terms "central" and "extremity solutions" were coined by Borri *et al.* [2, 14]; these two types of solutions are associated with the zero and non-vanishing eigenvalues of the Hamiltonian matrix, respectively, and are to be expected as a consequence of Saint-Venant's principle [19, 1]. Extremity solutions can be viewed as boundary layer solutions. Clearly, the determination of the central solutions is important, because they affect the beam's entire span as opposed to the extremity solutions that affect its ends only.

In this work, the solution of system (36) is obtained via structure preserving transformations. Consider a coordinate transformation of the following form

$$\underline{\hat{\mathcal{X}}} = \underline{\underline{\mathcal{S}}}\,\underline{\mathcal{Q}}, \tag{41}$$

where $\underline{\underline{\mathcal{S}}}$ is a yet undetermined symplectic matrix of size $2n \times 2n$ and $\underline{\mathcal{Q}}$ an array of $2n$ modal coordinates. Introducing this coordinate transformation into eq. (36) then yields $\underline{\mathcal{Q}}' = \underline{\underline{\bar{\mathcal{H}}}}_r\,\underline{\mathcal{Q}}$, where $\underline{\underline{\bar{\mathcal{H}}}}_r = \underline{\underline{\mathcal{S}}}^{-1}\underline{\underline{\bar{\mathcal{H}}}}\,\underline{\underline{\mathcal{S}}}$ is still a Hamiltonian matrix, as implied by property (85). Through a careful selection of the symplectic transformation matrix $\underline{\underline{\mathcal{S}}}$, the reduced Hamiltonian matrix, $\underline{\underline{\bar{\mathcal{H}}}}_r$, will become sparse, easing the solution of the reduced equations and enabling the explicit separation of the solution into its central and extremity components.

The existence of the zero eigenvalue is easy to prove. Indeed, identities (39) can be recast as

$$\underline{\underline{\bar{\mathcal{H}}}}\,\underline{\underline{\mathcal{Z}}} = -\underline{\underline{\mathcal{Z}}}\,\tilde{\tilde{\mathcal{K}}}^*, \tag{42}$$

where matrix $\underline{\underline{\mathcal{Z}}}$ is defined by eq. (38). For straight beams, four columns of matrix $\tilde{\tilde{\mathcal{K}}}^*$ vanish, which implies that Hamiltonian matrix $\underline{\underline{\bar{\mathcal{H}}}}$ is at least four times singular and the corresponding columns of matrix $\underline{\underline{\mathcal{Z}}}$ store the associated eigenvectors, which are, as expected, the beam's rigid-body motions. Note that the stiffness matrix of the structure is six times singular due to the presence of six rigid-body modes. The Hamiltonian matrix does not share this property.

4 Reduction of the Hamiltonian matrix

As indicated earlier, the Hamiltonian of the system will be reduced to a nearly diagonal form through the use of a coordinate transformations characterized by a symplectic matrix. For convenience, this process is broken into two steps. In section 4.1, it is assumed that the Hamiltonian possesses non-vanishing eigenvalues only and the corresponding extremity solutions provide the desired symplectic matrix. In section 4.2, the more difficult case of the vanishing eigenvalue is addressed and the associated central solutions lead to the desired transformation.

4.1 Extremity solutions

The extremity solutions are associated with the eigenvalues of Hamiltonian matrix $\underline{\underline{\bar{\mathcal{H}}}}$ with a non-vanishing real part, $\Re(\lambda_i) \neq 0$. Numerical tools are used to extract these eigenvalues and associated eigenvectors. As proved in section A.1, these eigenvalues occur in pairs of opposite sign, $\pm\lambda_i$, where $+\lambda_i$ indicates the eigenvalue with a positive real part. Because the Hamiltonian is a real but unsymmetric matrix, complex eigenvalues are possible and will occur in pairs of complex conjugate roots, $\pm\lambda_i$ and $\pm\lambda_i^\dagger$, where notation $(\cdot)^\dagger$ indicates a complex conjugate number. The following matrix is constructed with all the eigenvectors of the Hamiltonian

$$\underline{\underline{\mathcal{U}}}_e = \left[\underline{\mathcal{U}}_{-\lambda_1}, \cdots, \underline{\mathcal{U}}_{-\lambda_n}, \underline{\mathcal{U}}_{+\lambda_1}, \cdots, \underline{\mathcal{U}}_{+\lambda_n}\right]. \tag{43}$$

Equation (80) now expands to $\underline{\underline{\mathcal{U}}}_e^T\,\underline{\underline{\mathcal{J}}}\,\underline{\underline{\mathcal{U}}}_e = \underline{\underline{\mathcal{J}}}$, which, in view of eq. (82), implies that $\underline{\underline{\mathcal{U}}}_e$ is a symplectic matrix. Because the inverse of a symplectic matrix is given by eq. (83), it follows that $\underline{\underline{\mathcal{U}}}_e^{-1}\underline{\underline{\bar{\mathcal{H}}}}\,\underline{\underline{\mathcal{U}}}_e = \underline{\underline{\mathcal{J}}}^T\underline{\underline{\mathcal{U}}}_e^T\,\underline{\underline{\mathcal{J}}}\,\underline{\underline{\bar{\mathcal{H}}}}\,\underline{\underline{\mathcal{U}}}_e$ and introducing eq. (81) now leads to

$$\underline{\underline{\mathcal{U}}}_e^{-1}\underline{\underline{\bar{\mathcal{H}}}}\,\underline{\underline{\mathcal{U}}}_e = \begin{bmatrix} \mathrm{diag}(-\lambda_\alpha) & \underline{\underline{0}} \\ \underline{\underline{0}} & \mathrm{diag}(+\lambda_\alpha) \end{bmatrix} = \underline{\underline{\bar{\mathcal{H}}}}_e. \tag{44}$$

For the extremity solutions, the coordinate transformation expressed by eq. (41) becomes $\underline{\hat{\mathcal{X}}} = \underline{\underline{\mathcal{U}}}_e\,\underline{\mathcal{Q}}_e$. It involves symplectic matrix $\underline{\underline{\mathcal{U}}}_e$ and modal coordinates $\underline{\mathcal{Q}} = \underline{\mathcal{Q}}_e$, which can be interpreted

as the amplitudes of the extremity solution modes. As expected, the right-hand side of eq. (44) is a Hamiltonian matrix; it is also diagonal. The extremity solutions involve nodal force distributions that present no net resultant: they are self equilibrating, as expected from Saint-Venant's principle.

4.2 Central solutions

As for the extremity solutions, the central solutions are obtained from a coordinate transformation of the following type

$$\underline{\hat{\mathcal{X}}}_c = \underline{\underline{\mathcal{U}}}_c \underline{Q}_c, \tag{45}$$

where array $\underline{\hat{\mathcal{X}}}_c$ stores the nodal warping and force components associated with the central solution

$$\underline{\hat{\mathcal{X}}}_c = \begin{Bmatrix} \underline{\hat{u}}_c \\ \underline{\hat{P}}_c \end{Bmatrix}, \quad \underline{Q}_c = \begin{Bmatrix} \underline{\bar{\mathcal{U}}}^*_c \\ \underline{\bar{\mathcal{F}}}^*_c \end{Bmatrix}, \tag{46}$$

and array $\underline{Q}_c$ the canonical coordinates, $\underline{\bar{\mathcal{U}}}^*_c$ and $\underline{\bar{\mathcal{F}}}^*_c$, which will be identified as the average sectional displacements and stress resultants, respectively. The coordinate transformation is defined by matrix $\underline{\underline{\mathcal{U}}}_c$, which is partitioned as

$$\underline{\underline{\mathcal{U}}}_c = \begin{bmatrix} \underline{\underline{\bar{Z}}} & \underline{\underline{\bar{W}}} \\ \underline{\underline{0}} & \underline{\underline{\bar{Y}}} \end{bmatrix}, \tag{47}$$

where matrices $\underline{\underline{\bar{W}}}$ and $\underline{\underline{\bar{Y}}}$ are of size $n \times 6$ and yet undetermined.

The virtual work done by the nodal forces distributed over the beam's cross-section is obtained by multiplying the stress vector by the virtual displacement of its point of application, $\delta W = \underline{\hat{P}}_c^T \delta\underline{\hat{u}}$. In the present formulation, the virtual displacement consists of the rigid-section part, $\delta\underline{\hat{u}} = \underline{\underline{\bar{Z}}}\,\delta\underline{\bar{\mathcal{U}}}^*_R$, and of the warping part, $\delta\underline{\hat{u}} = \underline{\underline{\bar{Z}}}\,\delta\underline{\bar{\mathcal{U}}}^*_c + \underline{\underline{\bar{W}}}\,\delta\underline{\bar{\mathcal{F}}}^*_c$, leading to $\delta W = \underline{\bar{\mathcal{F}}}^{*T}_c \underline{\underline{\bar{Y}}}^T (\underline{\underline{\bar{Z}}}\,\delta\underline{\bar{\mathcal{U}}}^*_R + \underline{\underline{\bar{Z}}}\,\delta\underline{\bar{\mathcal{U}}}^*_c + \underline{\underline{\bar{W}}}\,\delta\underline{\bar{\mathcal{F}}}^*_c)$. If the following conditions are satisfied,

$$\underline{\underline{\bar{Y}}}^T \underline{\underline{\bar{Z}}} = \underline{\underline{I}}, \tag{48a}$$

$$\underline{\underline{\bar{Y}}}^T \underline{\underline{\bar{W}}} = \underline{\underline{0}}, \tag{48b}$$

the virtual work reduces to

$$\delta W = \underline{\hat{P}}_c^T (\underline{\underline{\bar{Z}}}\,\delta\underline{\mathcal{U}}^*_R + \delta\underline{\hat{u}}_c) = \underline{\bar{\mathcal{F}}}^{*T}_c (\delta\underline{\mathcal{U}}^*_R + \delta\underline{\bar{\mathcal{U}}}^*_c). \tag{49}$$

This implies that the canonical coordinates, $\underline{\bar{\mathcal{U}}}^*_c$ and $\underline{\bar{\mathcal{F}}}^*_c$, are energetically conjugated because their product yields the virtual work done by the distributed nodal forces exactly. Physically, the rigid-section motion, $\underline{\bar{\mathcal{U}}}^*_c$, is determined as the average warping of all nodes of the cross-section weighted by the nodal forces. It is verified easily that conditions (48) are sufficient to prove that matrix $\underline{\underline{\mathcal{U}}}_c$ defining the coordinate transformation (45) is symplectic, as desired.

Pre-multiplying eq. (45) by $\underline{\underline{\mathcal{U}}}_c^T \underline{\underline{\mathcal{J}}}$ and invoking the symplectic nature of matrix $\underline{\underline{\mathcal{U}}}_c$ leads to

$$\underline{\bar{\mathcal{F}}}^*_c = \underline{\underline{\bar{Z}}}^T \underline{\hat{P}}_c, \tag{50a}$$

$$\underline{\bar{\mathcal{U}}}^*_c = \underline{\underline{\bar{Y}}}^T \underline{\hat{u}}_c. \tag{50b}$$

Equation (50a) simply echoes eq. (40) and implies that canonical coordinates $\underline{\bar{\mathcal{F}}}^*_c$ are the stress resultants associated with the central solution. By construction, canonical coordinates $(\underline{\mathcal{U}}^*_R + \underline{\bar{\mathcal{U}}}^*_c)$, defined by eq. (50b), are energetically conjugated to the stress resultants.

Consider now the following transformation of the system's Hamiltonian matrix

$$\underline{\underline{\bar{\mathcal{H}}}}\,\underline{\underline{\mathcal{U}}}_c = \underline{\underline{\mathcal{U}}}_c \begin{bmatrix} -\tilde{\bar{\mathcal{K}}}^* & \underline{\underline{\bar{S}}}^* \\ \underline{\underline{0}} & \tilde{\bar{\mathcal{K}}}^{*T} \end{bmatrix} = \underline{\underline{\mathcal{U}}}_c \underline{\underline{\bar{\mathcal{H}}}}_c, \tag{51}$$

The first six columns of matrix $\underline{\underline{\bar{\mathcal{H}}}}_c$ simply echo relationship (42). Because matrix $\underline{\underline{\mathcal{U}}}_c$ is symplectic, matrix $\underline{\underline{\bar{\mathcal{H}}}}_c$ must be Hamiltonian, see eq. (85), and its general structure is given by eq. (77). This implies that the lower-right partition of $\underline{\underline{\bar{\mathcal{H}}}}_c$ equals $\tilde{\bar{\mathcal{K}}}^{*T}$ and its upper-right partition, denoted $\underline{\underline{\bar{S}}}^*$, is symmetric. Matrix $\underline{\underline{\bar{S}}}^*$ will be interpreted later as the sectional compliance matrix.

The existence of matrices $\underline{\underline{\bar{W}}}$, $\underline{\underline{\bar{Y}}}$, and $\underline{\underline{\bar{S}}}^*$ verifying eq. (51) and satisfying constraints (48a) and (48b) will now be proved. Introducing the explicit expression of the Hamiltonian matrix, eq. (37), into system (51) yields two matrix equations,

$$\underline{\underline{\bar{Y}}} = \underline{\underline{\bar{C}}}^T \underline{\underline{\bar{W}}} + \underline{\underline{\bar{M}}}\,\underline{\underline{\bar{Z}}}\,\underline{\underline{\bar{S}}}^* + \underline{\underline{\bar{M}}}\,\underline{\underline{\bar{W}}}\,\tilde{\bar{\mathcal{K}}}^{*T}, \tag{52a}$$

$$\underline{\underline{\bar{E}}}\,\underline{\underline{\bar{W}}} = \underline{\underline{\bar{Y}}}\,\tilde{\bar{\mathcal{K}}}^{*T} - \underline{\underline{\bar{C}}}\,\underline{\underline{\bar{Z}}}\,\underline{\underline{\bar{S}}}^* - \underline{\underline{\bar{C}}}\,\underline{\underline{\bar{W}}}\,\tilde{\bar{\mathcal{K}}}^{*T}. \tag{52b}$$

First, the sectional compliance matrix is expressed in terms of $\underline{\underline{\bar{W}}}$ by pre-multiplying eq. (52a) by $\underline{\underline{\bar{Z}}}^T$ and using condition (48a) to find

$$\underline{\underline{\bar{S}}}^* = \underline{\underline{\bar{F}}} \left[\underline{I} - (\underline{\underline{\bar{C}}}\,\underline{\underline{\bar{Z}}})^T \underline{\underline{\bar{W}}} - (\underline{\underline{\bar{M}}}\,\underline{\underline{\bar{Z}}})^T \underline{\underline{\bar{W}}}\,\tilde{\bar{\mathcal{K}}}^{*T} \right]. \tag{53}$$

where the flexibility matrix is defined as $\underline{\underline{\bar{F}}} = (\underline{\underline{\bar{Z}}}^T \underline{\underline{\bar{M}}}\,\underline{\underline{\bar{Z}}})^{-1}$.

Next, matrix $\underline{\underline{\bar{Y}}}$ is expressed in terms of $\underline{\underline{\bar{W}}}$ by introducing the sectional compliance matrix (53) into eqs. (52a) leading to eq. (54a). Finally, the governing equation for $\underline{\underline{\bar{W}}}$ is found by introducing eqs. (53) and (54a) into eq. (52b), leading to

$$\underline{\underline{\bar{Y}}} = \underline{\underline{\hat{C}}}^T \underline{\underline{\bar{W}}} + \underline{\underline{\hat{M}}}\,\underline{\underline{\bar{Z}}}\,\tilde{\bar{\mathcal{K}}}^{*T} + (\underline{\underline{\bar{M}}}\,\underline{\underline{\bar{Z}}})\underline{\underline{\bar{F}}}, \tag{54a}$$

$$\underline{\underline{\hat{M}}}\,\underline{\underline{\bar{W}}}\,\tilde{\bar{\mathcal{K}}}^{*T}\tilde{\bar{\mathcal{K}}}^{*T} - \underline{\underline{\hat{G}}}\,\underline{\underline{\bar{W}}}\,\tilde{\bar{\mathcal{K}}}^{*T} - \underline{\underline{\hat{E}}}\,\underline{\underline{\bar{W}}} = -\underline{\underline{\bar{V}}}, \tag{54b}$$

where the following notation was introduced

$$\underline{\underline{\hat{M}}} = \underline{\underline{\bar{M}}} - (\underline{\underline{\bar{M}}}\,\underline{\underline{\bar{Z}}})\underline{\underline{\bar{F}}}(\underline{\underline{\bar{M}}}\,\underline{\underline{\bar{Z}}})^T, \tag{55a}$$

$$\underline{\underline{\hat{C}}} = \underline{\underline{\bar{C}}} - (\underline{\underline{\bar{C}}}\,\underline{\underline{\bar{Z}}})\underline{\underline{\bar{F}}}(\underline{\underline{\bar{M}}}\,\underline{\underline{\bar{Z}}})^T, \tag{55b}$$

$$\underline{\underline{\hat{E}}} = \underline{\underline{\bar{E}}} - (\underline{\underline{\bar{C}}}\,\underline{\underline{\bar{Z}}})\underline{\underline{\bar{F}}}(\underline{\underline{\bar{C}}}\,\underline{\underline{\bar{Z}}})^T, \tag{55c}$$

$$\underline{\underline{\bar{V}}} = (\underline{\underline{\bar{M}}}\,\underline{\underline{\bar{Z}}})\underline{\underline{\bar{F}}}\tilde{\bar{\mathcal{K}}}^{*T} - (\underline{\underline{\bar{C}}}\,\underline{\underline{\bar{Z}}})\underline{\underline{\bar{F}}}, \tag{55d}$$

and $\underline{\underline{\hat{G}}} = \underline{\underline{\hat{C}}} - \underline{\underline{\hat{C}}}^T$. With the help of identities (39), it is shown easily that

$$\underline{\underline{\bar{Z}}}^T \underline{\underline{\hat{M}}} = \underline{\underline{\bar{Z}}}^T \underline{\underline{\hat{G}}} = \underline{\underline{\bar{Z}}}^T \underline{\underline{\hat{E}}} = \underline{\underline{0}}, \tag{56}$$

which proves that matrices $\underline{\underline{\hat{M}}}$, $\underline{\underline{\hat{G}}}$, and $\underline{\underline{\hat{E}}}$ are six times singular and matrix $\underline{\underline{\bar{Z}}}$ spans their null space. Furthermore, it is also true that

$$\underline{\underline{\bar{Z}}}^T \underline{\underline{\bar{V}}} = \underline{\underline{0}}. \tag{57}$$

System (54b) provides $6n$ equations for the $6n$ unknown components of matrix $\underline{\underline{\bar{W}}}$, but all matrices of the system are six times singular. Bauchau and Han [12] have shown that this system is solvable for the straight-beam case. To ease the solution of the curved-beam case, a transformation

of the generalized vector-product tensor defined by eq. (8) is introduced. Let $\tilde{\tilde{\mathcal{K}}} = \underline{\underline{\mathcal{C}}}^{-1}\tilde{\tilde{\mathcal{K}}}^{*}\underline{\underline{\mathcal{C}}}$, where $\underline{\underline{\mathcal{C}}}$ is the motion tensor defined as

$$\underline{\underline{\mathcal{C}}} = \begin{bmatrix} \underline{\underline{R}} & \tilde{u}\underline{\underline{R}} \\ \underline{\underline{0}} & \underline{\underline{R}} \end{bmatrix}, \tag{58}$$

$\underline{\underline{R}}$ an orthogonal rotation tensor and $\underline{u}$ a displacement vector. These two quantities will be selected to obtain a simplified form of the generalized vector-product tensor,

$$\tilde{\tilde{\mathcal{K}}} = \begin{bmatrix} \bar{\kappa}\,\tilde{\imath}_1 & \tau\,\tilde{\imath}_1 \\ \underline{\underline{0}} & \bar{\kappa}\,\tilde{\imath}_1 \end{bmatrix}, \tag{59}$$

where $\bar{\imath}_1^T = \{1, 0, 0\}$. Simple algebra reveals that $\bar{\kappa}^2\underline{u} = \tilde{\kappa}^*\underline{t}^*$, where $\bar{\kappa} = \|\underline{\bar{\kappa}}^*\|$, $\bar{\kappa}\tau = \underline{\bar{\kappa}}^{*T}\underline{t}^*$, and the rotation tensor is expressed as $\underline{\underline{R}} = [\bar{e}_1, \bar{e}_2, \bar{e}_3]$, where unit vector $\bar{e}_1 = \underline{\bar{\kappa}}^*/\bar{\kappa}$, and mutually orthogonal unit vectors $\bar{e}_2$ and $\bar{e}_3$ can be selected arbitrarily in the plane perpendicular to $\bar{e}_1$.

System (54b) now transforms to

$$\underline{\underline{\hat{M}}}\,\underline{\underline{\bar{W}}}^{\flat}\tilde{\tilde{\mathcal{K}}}^T\tilde{\tilde{\mathcal{K}}}^T - \underline{\underline{\hat{G}}}\,\underline{\underline{\bar{W}}}^{\flat}\tilde{\tilde{\mathcal{K}}}^T - \underline{\underline{\hat{E}}}\,\underline{\underline{\bar{W}}}^{\flat} = -\underline{\underline{\bar{V}}}^{\flat}, \tag{60}$$

where $\underline{\underline{\bar{W}}}^{\flat} = \underline{\underline{\bar{W}}}\,\underline{\underline{\mathcal{C}}}^{-T}$, $\underline{\underline{\bar{V}}}^{\flat} = \underline{\underline{\bar{V}}}\,\underline{\underline{\mathcal{C}}}^{-T}$. The solution of system (60) now breaks down into three uncoupled problems, which can be solved recursively

$$\underline{\underline{\hat{E}}}\,[\underline{w}_1^{\flat}, \underline{w}_4^{\flat}] = [\underline{v}_1^{\flat}, \underline{v}_4^{\flat}], \tag{61a}$$

$$\begin{bmatrix} \underline{\underline{\hat{E}}} + \bar{\kappa}^2\underline{\underline{\hat{M}}} & -\bar{\kappa}\underline{\underline{\hat{G}}} \\ \bar{\kappa}\underline{\underline{\hat{G}}} & \underline{\underline{\hat{E}}} + \bar{\kappa}^2\underline{\underline{\hat{M}}} \end{bmatrix} \begin{Bmatrix} \underline{w}_5^{\flat} \\ \underline{w}_6^{\flat} \end{Bmatrix} = \begin{Bmatrix} \underline{v}_5^{\flat} \\ \underline{v}_6^{\flat} \end{Bmatrix}, \tag{61b}$$

$$\begin{bmatrix} \underline{\underline{\hat{E}}} + \bar{\kappa}^2\underline{\underline{\hat{M}}} & -\bar{\kappa}\underline{\underline{\hat{G}}} \\ \bar{\kappa}\underline{\underline{\hat{G}}} & \underline{\underline{\hat{E}}} + \bar{\kappa}^2\underline{\underline{\hat{M}}} \end{bmatrix} \begin{Bmatrix} \underline{w}_2^{\flat} \\ \underline{w}_3^{\flat} \end{Bmatrix} = \begin{Bmatrix} \underline{v}_2^{\flat} - 2\tau\bar{\kappa}\underline{\underline{\hat{M}}}\,\underline{w}_5^{\flat} + \tau\underline{\underline{\hat{G}}}\,\underline{w}_6^{\flat} \\ \underline{v}_3^{\flat} - \tau\underline{\underline{\hat{G}}}\,\underline{w}_5^{\flat} - 2\tau\bar{\kappa}\underline{\underline{\hat{M}}}\,\underline{w}_6^{\flat} \end{Bmatrix}. \tag{61c}$$

Here again, the three subproblems are singular but solvable, because eqs (56) and (57) provide the solvability conditions.

4.2.1 The sectional compliance matrix

For either straight- or curved-beam cases, matrix $\underline{\underline{\bar{W}}}$ can be determined using the procedure outlined above. Because the systems are singular, the general solutions can be written as $\underline{\underline{\bar{W}}} = \underline{\underline{\bar{W}}}^{\natural} + \underline{\underline{\bar{Z}}}\,\underline{\alpha}$, where $\underline{\underline{\bar{W}}}^{\natural}$ is a particular solution of the problem. Because the solution must satisfy condition (48b), coefficients $\underline{\alpha}$ are found easily as $\underline{\alpha} = -\underline{\underline{\bar{Y}}}^T\,\underline{\underline{\bar{W}}}^{\natural}$.

Equation (54a) now gives matrix $\underline{\underline{\bar{Y}}}$, which is independent of coefficients $\underline{\alpha}$. Finally, eq. (53) yields the sectional compliance matrix as

$$\underline{\underline{\bar{S}}}^{*} = \underline{\underline{\bar{S}}}^{\natural} - \tilde{\tilde{\mathcal{K}}}^{*}\underline{\alpha} - \underline{\alpha}\,\tilde{\tilde{\mathcal{K}}}^{*T}, \tag{62}$$

where $\underline{\underline{\bar{S}}}^{\natural} = \underline{\underline{\bar{F}}}[\underline{\underline{I}} - (\underline{\underline{\bar{C}}}\,\underline{\bar{Z}})^T\underline{\underline{\bar{W}}}^{\natural} - (\underline{\underline{\bar{M}}}\,\underline{\bar{Z}})^T\underline{\underline{\bar{W}}}^{\natural}\tilde{\tilde{\mathcal{K}}}^{*T}]$.

4.3 Complete solution

The coordinate transformations defined in the two previous sections are now combined into a single transformation $\hat{\underline{\mathcal{X}}} = \underline{\underline{\mathcal{U}}}\,\underline{\mathcal{Q}} = [\underline{\underline{\mathcal{U}}}_c \;\; \underline{\underline{\mathcal{U}}}_e]\,\underline{\mathcal{Q}}$, where array $\underline{\mathcal{Q}}^T = \{\underline{\mathcal{Q}}_c^T, \underline{\mathcal{Q}}_e^T\}$ stores the generalized coordinates associated with the central and extremity solutions. Because matrix $\underline{\underline{\mathcal{U}}}$ is symplectic, the following transformation results

$$\underline{\underline{\mathcal{U}}}^{-1}\underline{\underline{\bar{\mathcal{H}}}}\,\underline{\underline{\mathcal{U}}} = \underline{\underline{\hat{\mathcal{H}}}} = \begin{bmatrix} \underline{\underline{\bar{\mathcal{H}}}}_c & \underline{\underline{0}} \\ \underline{\underline{0}} & \underline{\underline{\bar{\mathcal{H}}}}_e \end{bmatrix}. \tag{63}$$

Note that the reduced system Hamiltonian is now in nearly diagonal form, easing the solution of the problem.

5 Three-dimensional beam solutions

The reduced governing equations of the problem given by eq. (63) are now fully defined and because the central and extremity solutions are decoupled, their solutions can be derived independently.

5.1 Extremity solutions

Because the portion of the Hamiltonian pertaining to the extremity solutions is diagonal, see eq. (44), the governing equations for the generalized coordinates are of the form $q'_{+\lambda_i} = \bar{\lambda}_i q_{+\lambda_i}$ and their solutions are $q_{+\lambda_i} = \ell \exp(+\bar{\lambda}_i \bar{\alpha}_1)$. The corresponding analytical solution in the physical domain is then obtained easily

$$\underline{\hat{\mathcal{X}}}_e(\bar{\alpha}_1) = \sum_{i=1}^{N_e} \left[e^{+\bar{\lambda}_i \bar{\alpha}_1} \underline{\mathcal{U}}_{+\lambda_i} \ell_{+\lambda_i} + e^{-\bar{\lambda}_i \bar{\alpha}_1} \underline{\mathcal{U}}_{-\lambda_i} \ell_{-\lambda_i} \right], \tag{64}$$

where $N_e = n - 6$ is the number of extremity solutions, and $\ell_{+\lambda_i}$ and $\ell_{-\lambda_i}$ are integration constants to be evaluated from the boundary conditions. Clearly, these solutions are exponentially decaying solutions emanating from the beam's ends.

5.2 Central solution

Projection of the governing eqs. (36) onto the modal space of the central solution yields the governing system for the twelve canonical coordinates,

$$\begin{Bmatrix} \bar{\underline{\mathcal{U}}}_c^* \\ \bar{\underline{\mathcal{F}}}_c^* \end{Bmatrix}' = \begin{bmatrix} -\tilde{\bar{\mathcal{K}}}^* & \bar{\underline{\underline{S}}}^* \\ \underline{\underline{0}} & \tilde{\bar{\mathcal{K}}}^{*T} \end{bmatrix} \begin{Bmatrix} \bar{\underline{\mathcal{U}}}_c^* \\ \bar{\underline{\mathcal{F}}}_c^* \end{Bmatrix} - \begin{Bmatrix} \bar{\underline{\mathcal{E}}}_R^* \\ \underline{0} \end{Bmatrix}, \tag{65}$$

The last six equations of this set provide the stress resultant equilibrium equations, $\bar{\underline{\mathcal{F}}}_c^{*\prime} - \tilde{\bar{\mathcal{K}}}^{*T} \bar{\underline{\mathcal{F}}}_c^* = \underline{0}$. The first six equations define the sectional constitutive laws relating the stress resultants, $\bar{\underline{\mathcal{F}}}_c^*$, to the sectional strains as $\bar{\underline{\mathcal{E}}}_c^* = \bar{\underline{\underline{S}}}^* \bar{\underline{\mathcal{F}}}_c^* = \bar{\underline{\mathcal{U}}}_c^{*\prime} + \tilde{\bar{\mathcal{K}}}^* \bar{\underline{\mathcal{U}}}_c^* + \bar{\underline{\mathcal{E}}}_R^*$. The sectional strains due to warping are defined as

$$\bar{\underline{\mathcal{E}}}_W^* = \bar{\underline{\mathcal{U}}}_c^{*\prime} + \tilde{\bar{\mathcal{K}}}^* \bar{\underline{\mathcal{U}}}_c^*, \tag{66}$$

and the sectional constitutive laws become $\bar{\underline{\mathcal{E}}}_c^* = \bar{\underline{\mathcal{E}}}_W^* + \bar{\underline{\mathcal{E}}}_R^* = \bar{\underline{\underline{S}}}^* \bar{\underline{\mathcal{F}}}_c^*$, where symmetric matrix $\bar{\underline{\underline{S}}}^*$ stores the components of the sectional compliance matrix resolved in the material basis. The governing equations of the central solutions are recast as

$$\bar{\underline{\mathcal{F}}}_c^{*\prime} - \tilde{\bar{\mathcal{K}}}^{*T} \bar{\underline{\mathcal{F}}}_c^* = \underline{0}, \tag{67a}$$

$$\bar{\underline{\mathcal{E}}}_c^* - \bar{\underline{\underline{S}}}^* \bar{\underline{\mathcal{F}}}_c^* = \underline{0}. \tag{67b}$$

From the onset of the formulation, the displacement field was divided into a rigid-section motion and a warping field. This decomposition facilitates the analytical developments, but is of course, a view of the mind. Indeed, when expressing the constitutive laws, the total strain only, $\bar{\underline{\mathcal{E}}}_c^* = \bar{\underline{\mathcal{E}}}_W^* + \bar{\underline{\mathcal{E}}}_R^*$, is important, as it relates to the stress resultants.

5.2.1 Geometrically exact beam equations

To complete the formulation, a set of strain-displacement relationships must be derived. To that effect, the following rigid-section motion tensor is defined

$$\underline{\underline{\mathcal{C}}}(\alpha_1) = \begin{bmatrix} (\underline{\underline{R}}_c \underline{\underline{R}} \underline{\underline{R}}_0) & (\tilde{R}_{B_R} + \tilde{u}_c)(\underline{\underline{R}}_c \underline{\underline{R}} \underline{\underline{R}}_0) \\ \underline{\underline{0}} & (\underline{\underline{R}}_c \underline{\underline{R}} \underline{\underline{R}}_0) \end{bmatrix}. \tag{68}$$

It combines the rigid-section motion represented by motion tensor (7) with the additional rigid-body motion included in the warping field. The generalized coordinates of the central solutions, $\underline{\mathcal{U}}_c^{*T} = \{\underline{u}_c^{*T}, \underline{\phi}_c^{*T}\}$, involve a set of displacement components, $\underline{u}_c^*$, and a set of rotations, $\underline{\phi}_c^*$. Both sets are of small magnitude because the warping is itself small, and hence, the rotation tensor appearing in eq. (68) is approximated as $\underline{\underline{R}}_c \approx \underline{\underline{I}} + \tilde{\phi}_c$.

The components of the beam's curvature vector in its deformed configuration are $\tilde{\mathcal{L}}^* = \underline{\underline{\mathcal{C}}}^{-1}\underline{\underline{\mathcal{C}}}'$, and

$$\underline{\mathcal{L}}^* = \begin{Bmatrix} (\underline{\underline{R}}_c \underline{\underline{R}} \underline{\underline{R}}_0)^T (\underline{R}'_{B_R} + \underline{u}'_c) \\ \text{axial}((\underline{\underline{R}}_c \underline{\underline{R}} \underline{\underline{R}}_0)^T (\underline{\underline{R}}_c \underline{\underline{R}} \underline{\underline{R}}_0)') \end{Bmatrix} = \begin{Bmatrix} \bar{T}^* + (\underline{\underline{R}} \underline{\underline{R}}_0)^T \underline{u}'_c + \tilde{\phi}_c^{*T} \bar{T}^* \\ \bar{K}^* + (\underline{\underline{R}} \underline{\underline{R}}_0)^T \underline{\phi}'_c \end{Bmatrix}, \tag{69}$$

where the second equality results from introducing approximation $\underline{\underline{R}}_c \approx \underline{\underline{I}} + \tilde{\phi}_c$ and neglecting higher-order terms. Using eq. (66) then results in $\underline{\mathcal{L}}^* - \bar{\underline{k}}_0^+ = \underline{\mathcal{E}}_R^* + \underline{\mathcal{E}}_W^* = \underline{\mathcal{E}}_c^*$, leading to the following strain-displacement relationships,

$$\bar{\underline{\mathcal{E}}}_c^* = \begin{Bmatrix} \underline{\epsilon}_c^* \\ \bar{\underline{\varkappa}}_c^* \end{Bmatrix} = \begin{Bmatrix} (\underline{\underline{\mathcal{R}}} \underline{\underline{R}}_0)^T \underline{\bar{R}}'_c - \bar{t}^+ \\ \underline{\underline{\bar{R}}}_0^T \text{axial}(\underline{\underline{\mathcal{R}}}^T \underline{\underline{\mathcal{R}}}') \end{Bmatrix}, \tag{70}$$

whose form is identical to that of eq. (17). In these equations, $\underline{R}_c = \underline{R}_{B_R} + \underline{u}_c$ approximates the displacement of material point **B** shown in fig. 1; note that displacement $\underline{u}_c$ is small and hence, negligible compared to rigid-section displacement $\underline{R}_{B_R}$. Rotation tensor $\underline{\underline{\mathcal{R}}} = \underline{\underline{R}}_c \underline{\underline{R}}$ is not the rotation of the "rigid cross-section," but rather, defines the average orientation of the deformed cross-section after warping. The strain energy equivalence (49) defines $\underline{u}_c$ and $\underline{\underline{R}}_c$.

In summary, eqs. (67a), (67b), and (70) are the equilibrium, constitutive, and strain-displacement equations, respectively, of the problem. It is interesting to note that these equations are the geometrically exact beam equations, first postulated by Simo and co-workers [20, 21]; similar developments were proposed by Borri and Merlini [14] or Danielson and Hodges [22, 15]. In all these references, the strain-displacement relationships (70) were postulated whereas in the present approach, these relationships were derived from three-dimensional elasticity. In general, no closed-form solutions of these equations exist and numerical tools, such as finite element method, should be used.

5.2.2 Detailed three-dimensional solution

The geometrically exact beam equations derived in the previous section describe the problem in terms of rigid-section motion tensor (68) together with the sectional strains and forces, $\bar{\underline{\mathcal{E}}}_c^*$ and $\bar{\underline{\mathcal{F}}}_c^*$, respectively.

Because it is based on three-dimensional elasticity, the present approach provides a far more detailed description of the solution. Indeed, eq. (45) now yields the nodal warping and force components associated with the central solution

$$\underline{\hat{u}}_c = \underline{\bar{Z}}\, \bar{\mathcal{U}}_c^* + \underline{\bar{W}}\, \bar{\underline{\mathcal{F}}}_c^*, \tag{71a}$$

$$\underline{\hat{P}}_c = \underline{\bar{Y}}\, \bar{\underline{\mathcal{F}}}_c^*. \tag{71b}$$

Nodal displacements (71a) involve two contributions: the first term accounts for rigid-section motion and the second for warping. The columns of matrix $\underline{\underline{\bar{W}}}$ represent the warping induced by unit sectional stress resultants. Note that eq. (71a) resolves the "double counting" of the rigid-body motions underlined in section 2.3. Indeed, eq. (54b) and condition (48b) define matrix $\underline{\underline{\bar{W}}}$ unambiguously. This warping field still contain a rigid-body motion and the first terms of eq. (71a) describes the rigid-body motion associated with the rigid-section motion, $\underline{\bar{\mathcal{U}}}_c^*$. Nodal forces (71b) depend on sectional stress resultants only; the columns of matrix $\underline{\underline{\bar{Y}}}$ represent the nodal forces induced by unit sectional stress resultants.

Furthermore, eq. (27) yields the six components of the strain tensor associated with the central solution as $\underline{\gamma}_c^* = \underline{\underline{\bar{A}}}\,\underline{\underline{N}}(\hat{\underline{u}}_c' + \underline{\underline{\bar{Z}}}\,\underline{\bar{\mathcal{E}}}_R^*) + \underline{\underline{\bar{B}}}\,\underline{\underline{N}}\,\hat{\underline{u}}_c$. Introducing the nodal displacement components (71a), their spatial derivative, and eq. (66) leads to $\underline{\gamma}_c^* = \underline{\underline{\bar{A}}}\,\underline{\underline{N}}[\underline{\underline{\bar{Z}}}(\underline{\bar{\mathcal{E}}}_R^* + \underline{\bar{\mathcal{E}}}_W^* - \tilde{\bar{\mathcal{K}}}^*\underline{\bar{\mathcal{U}}}_c^*) + \underline{\underline{\bar{W}}}\,\underline{\bar{\mathcal{F}}}_c^{*\prime}] + \underline{\underline{\bar{B}}}\,\underline{\underline{N}}\,(\underline{\underline{\bar{Z}}}\,\underline{\bar{\mathcal{U}}}_c^* + \underline{\underline{\bar{W}}}\,\underline{\bar{\mathcal{F}}}_c^*)$. Regrouping terms yields $\underline{\gamma}_c^* = \underline{\underline{\bar{A}}}\,\underline{\underline{N}}[\underline{\underline{\bar{Z}}}\,\underline{\bar{\mathcal{E}}}_c^* + \underline{\underline{\bar{W}}}\,\underline{\bar{\mathcal{F}}}_c^{*\prime}] + \underline{\underline{\bar{B}}}\,\underline{\underline{N}}\,\underline{\underline{\bar{W}}}\,\underline{\bar{\mathcal{F}}}_c^* + (\underline{\underline{\bar{B}}}\,\underline{\underline{N}}\,\underline{\underline{\bar{Z}}} - \underline{\underline{\bar{A}}}\,\underline{\underline{N}}\,\underline{\underline{\bar{Z}}}\tilde{\bar{\mathcal{K}}}^*)\underline{\bar{\mathcal{U}}}_c^*$. The last term vanishes because rigid-body displacements create no strains; the sectional equilibrium equations (67a) then yield

$$\underline{\gamma}_c^* = \left[\underline{\underline{\bar{A}}}\,\underline{\underline{N}}(\underline{\underline{\bar{Z}}}\,\underline{\bar{S}}^* + \underline{\underline{\bar{W}}}\,\tilde{\bar{\mathcal{K}}}^{*T}) + \underline{\underline{\bar{B}}}\,\underline{\underline{N}}\,\underline{\underline{\bar{W}}}\right]\underline{\mathcal{F}}_c^*, \tag{72}$$

Finally, the three-dimensional stress tensor is obtained from the constitutive laws (29) as $\underline{\tau}_c^* = \underline{\underline{\mathcal{D}}}^*\underline{\gamma}_c^*$. Equation (72) implies that the complete three-dimensional strain field at any point of the cross-section can be expressed in terms of the six sectional stress resultants only.

5.2.3 Discussion

The previous sections have presented a nonlinear theory for three-dimensional beam problems. Kinematically, the problem was decomposed into a rigid-section motion and a warping field. The sectional strains associated with rigid-section motion and the warping field were assumed to remain small at all times. As a natural consequence of this kinematic decomposition, the governing equations of the problem fall into two distinct categories: the equations describing geometrically exact beams, see section 5.2.1, and those describing local deformations, see section 5.2.2.

The average rigid-section motions of geometrically exact beams are governed by nonlinear, one-dimensional equations, whereas a linear, two-dimensional analysis provides the detailed distribution of three-dimensional stresses and strains. A similar decomposition was obtained by Hodges and his co-workers [23, 24] based on variational asymptotic arguments.

The decomposition of the problem into two simpler problems is not an assumption. Rather, the present developments show that it is a natural consequence of the proposed kinematic description of the problem. The approach starts from the general theory of three-dimensional elasticity and makes two assumptions only: the sectional strains associated with rigid-section motion and warping displacement components remain very small at all times. Given these assumptions, the solutions presented here are exact solutions of three-dimensional elasticity for beams undergoing arbitrarily large motions, within the discretization error inherent to the finite element approach. Indeed, the proposed approach relies on a finite element discretization of the beam's cross-section.

The constitutive laws expressed by eq. (67b) play a key role in the present formulation and follow from the energy equivalence expressed by eq. (49). Indeed, variation in the strain energy stored in an infinitesimal slice of the beam of span $\mathrm{d}\alpha_1$, denoted δA, is found as the difference of the virtual work done by externally forces applied to two neighboring sections, leading to $\delta A = (\hat{\underline{P}}^T\delta\hat{\underline{u}})'$. For the deformation associated with the central solution, eq. (71b) implies $\delta A = [\underline{\mathcal{F}}_c^{*T}\underline{\underline{Y}}^T(\underline{\underline{Z}}\,\underline{\delta\mathcal{U}}_R^* + \delta\hat{\underline{u}}_c)]'$, where the first term in the parenthesis represents the contribution from the rigid-section motion and the second that of the warping. Introducing eq. (71a) and using conditions (48) then leads to $\delta A = [\underline{\mathcal{F}}_c^{*T}(\underline{\delta\mathcal{U}}_R^* + \delta\underline{\bar{\mathcal{U}}}_c^*)]'$. Expanding and using the equilibrium equations (67a) yields $\delta A =$

$\underline{\mathcal{F}}_c^{*T}(\underline{\delta\mathcal{U}}_R^{*\prime} + \tilde{\bar{\mathcal{K}}}^*\underline{\delta\mathcal{U}}_R^* + \underline{\delta\bar{\mathcal{U}}}_c^{*\prime} + \tilde{\bar{\mathcal{K}}}^*\underline{\delta\bar{\mathcal{U}}}_c^*) = \underline{\mathcal{F}}_c^{*T}(\underline{\delta\bar{\mathcal{E}}}_R^* + \underline{\delta\bar{\mathcal{E}}}_W^*)$, where the second equality follows from eqs. (24) and (66). Finally, $\delta A = \underline{\mathcal{F}}_c^{*T}\underline{\delta\bar{\mathcal{E}}}_c^*$, and introducing the sectional constitute laws (67b) yields $\delta A = \delta(\underline{\mathcal{F}}_c^{*T}\underline{\bar{\mathcal{S}}}^*\underline{\bar{\mathcal{F}}}_c^*)/2$.

In summary, the strain energy stored in a slice of the beam computed based on the detailed three-dimensional distribution of nodal forces and corresponding displacements exactly equals that expressed in terms of six stress resultants only. The proposed approach evaluates the compliance matrix based on this exact strain energy equivalence. Consequently, the compliance matrix obtained from the proposed approach is always symmetric and positive-definite; this result is not obvious, considering that eq. (62) is used to evaluate the compliance matrix. Furthermore, this exact strain energy equivalence renders coordinate transformation (47) symplectic, providing the desired structure preserving transformation. Once the sectional forces are obtained from equilibrium considerations, the energetically conjugate sectional strains follow from the constitutive laws (67b).

6 Numerical results

To validate the cross-sectional analysis procedure proposed in this paper, a set of numerical examples will be presented.

6.1 Thin-walled C-section beam

The first example deals with the thin-walled, C-section depicted in fig. 2. The top and bottom flanges are of width b and the web is height $h = 2b$. The walls of uniform thickness t are made of a homogenous, isotropic material of shear modulus G. Within the framework of thin-walled beam theory [1], analytical expressions are obtained for the section's torsional stiffness, $J_t/(Gbt^3) = (2 + h/b)/3$, shear center location, $e_t/b = 3/(6 + h/b)$, and tangential shear stress at point **A**, $bt^2\tau_t/M_1 = 3/(2 + h/b)$, where M_1 is the applied torque and point **A** is located at the mid-span of the flange, as indicated in fig. 2. These predictions are exact for thin-walled beam, *i.e.*, when $t/h \to 0$ and $t/b \to 0$.

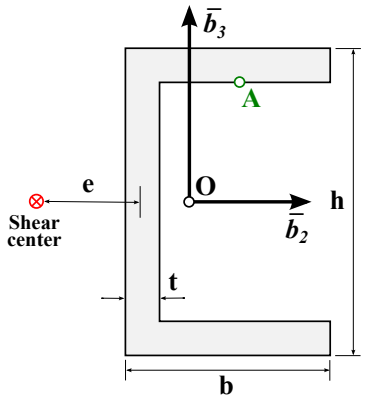

Figure 2: Configuration of the C-section beam.

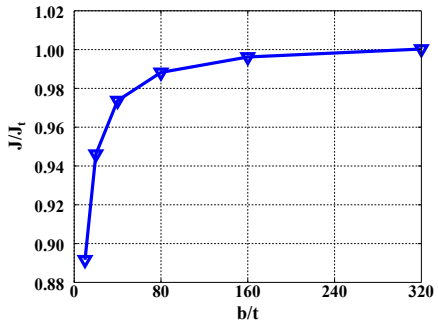

Figure 3: Non-dimensional torsional stiffness versus aspect ratio.

The proposed method was used to determine the central solution of the C-section. Nine-node quadrilateral elements arranged in 60×4, 40×4, and 40×4 grids were used to mesh the web, top flange, and bottom flange, respectively. Six different aspect ratio, b/t = 10, 20, 40, 80, 160, and 320, were considered. As this aspect ratio increases, the predictions of thin-walled beam theory become increasingly accurate. Based on the central solution, the section's torsional stiffness, shear center location, and tangential shear stress at point **A** are then obtained easily and are denoted J, e, and τ, respectively.

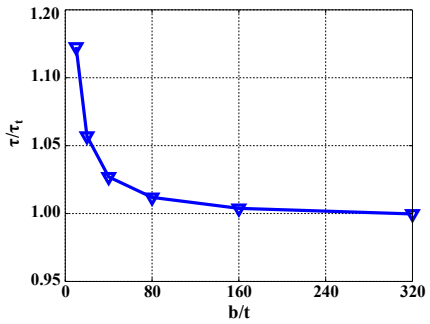

Figure 4: Non-dimensional maximum shear stress versus aspect ratio.

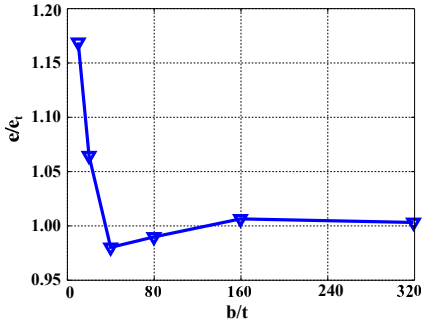

Figure 5: Non-dimensional location of the shear center versus aspect ratio.

Figure 3 depicts the torsional stiffness ratio, J/J_t, versus the aspect ratio, b/t. Note the convergence of the thin-walled beam theory predictions to those of the present approach. For thick sections, the torsional stiffness predicted by thin-walled beam is too high, as expected. The tangential shear stress ratio at point **A**, τ/τ_t, appears in fig. 4. Note that the predictions of thin-walled beam theory are not conservative. Finally, fig. 5 shows the shear center location ratio, e/e_t versus the aspect ratio b/t.

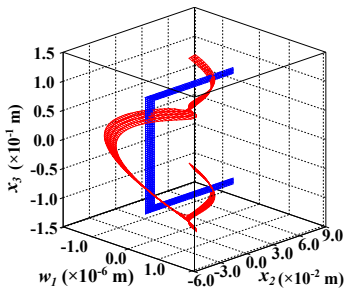

Figure 6: Out-of-plane warping component, w_1, due to a unit shear force applied at the shear center and acting along unit vector $\bar{b}_2$.

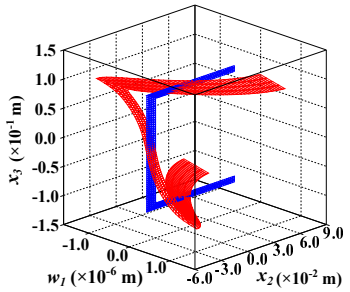

Figure 7: Out-of-plane warping component, w_1, due to a unit shear force applied at the shear center and acting along unit vector $\bar{b}_3$.

The proposed approach is based on the decomposition of the displacement field into a rigid-section motion and a warping field. The former is that used by Euler-Bernoulli theory and the latter, which characterizes the present approach, is obtained from three-dimensional elasticity. The warping fields due to unit stress resultants will be shown for a C-section of dimensions $h = 0.2$, $b = 0.1$, and $t = 0.01$ m. The mesh used here is the same as that described earlier. The warping fields generated by axial forces and bending moments are due to Poisson's effects only and will not be shown here. On the other hand, the warping fields due to unit transverse shear forces applied at the shear center and acting along unit vectors $\bar{b}_2$ and $\bar{b}_3$ are depicted in figs. (6) and (7), respectively. The in-plane warping components, w_2 and w_3, vanish; the figures show the out-of-plane warping component, w_1.

Finally, fig. (8) shows the out-of-plane warping component of the C-section subjected to a unit torque. The shape of this warping field is in good agreement with that predicted by thin-walled beam theory [1]. Note that the magnitude of this warping is much larger than those observed when the section is acted upon by transverse shear forces. Even for thin-walled beam theory, evaluation of the torsional stiffness is based on the warping field. The correct torsional stiffness of the beam cannot be obtained without first computing the warping field.

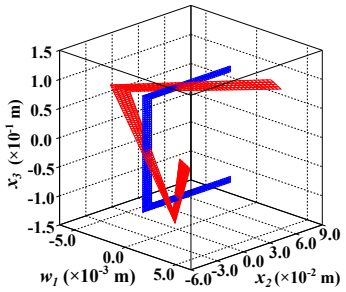

Figure 8: Out-of-plane warping component, w_1, due to a unit torque acting about $\bar{b}_1$.

6.2 Rectangular box section

The second example deals with the thin-walled, rectangular section depicted in fig. 9. The section is 0.753×0.537 in^2 and was the object of numerical and analytical studies carried out by Borri *et al.* [25]. The walls consist of six, 0.005 in thick plies of graphite/epoxy material with the following material properties: longitudinal modulus $E_L = 20.59$ Msi, transverse modulus $E_T = 1.42$ Msi, shearing modulus $G_{LT} = 0.87$ Msi, and Poisson's ratios $\nu_{LT} = \nu_{TN} = 0.42$.

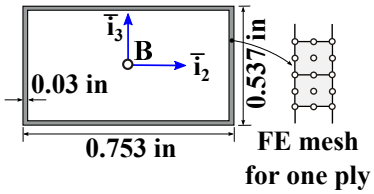

Figure 9: Thin walled box section.

Six different lay-ups, described in Table 1, were considered. Lay-up definitions start with the innermost ply and end with the outermost ply; 0° fibers are aligned with the axis of the beam and a positive ply angle indicates a right-hand rotation about the local normal to the thin wall. For this problem, 40×6 quadrilateral, nine-node elements were used to mesh the longer walls and 20×6 to mesh the shorter walls of the section. The mesh for a single ply of the wall is depicted in fig. 9.

Table 1: Definition of the six lay-ups

Lay-up type	Upper wall	Lower wall	Left wall	Right wall
1	$[15^\circ_6]$	$[15^\circ_6]$	$[15^\circ_6]$	$[15^\circ_6]$
2	$[0^\circ, 30^\circ]_3$	$[0^\circ, 30^\circ]_3$	$[0^\circ, 30^\circ]_3$	$[0^\circ, 30^\circ]_3$
3	$[0^\circ, 45^\circ]_3$	$[0^\circ, 45^\circ]_3$	$[0^\circ, 45^\circ]_3$	$[0^\circ, 45^\circ]_3$
4	$[15^\circ]_6$	$[-15^\circ]_6$	$[15^\circ, -15^\circ]_3$	$[-15^\circ, 15^\circ]_3$
5	$[30^\circ]_6$	$[-30^\circ]_6$	$[30^\circ, -30^\circ]_3$	$[-30^\circ, 30^\circ]_3$
6	$[45^\circ]_6$	$[-45^\circ]_6$	$[45^\circ, -45^\circ]_3$	$[-45^\circ, 45^\circ]_3$

Table 2 lists two components of the compliance matrix, S_{55} and S_{44}, which represent the bending and torsional compliances of the section, respectively. Table 3 lists two additional components of the compliance matrix, S_{14} and S_{45}, which represent the extension-torsion and bending-torsion coupling compliances, respectively. For comparison, the results obtained by Borri *et al.* [25] are also presented in the tables. Clearly, the two sets of predictions are in good agreement. The small discrepancies are likely to be due to the different meshes and shape functions used in the two analyses.

Table 2: Bending and torsional components of the compliance matrix. Borri *et al.*: $(\cdot)^B$, present predictions: $(\cdot)^P$.

Lay-up	$S^B_{55}\times 10^5$ $[\text{lbs}\cdot\text{in}^2]^{-1}$	$S^P_{55}\times 10^5$ $[\text{lbs}\cdot\text{in}^2]^{-1}$	$S^B_{44}\times 10^5$ $[\text{lbs}\cdot\text{in}^2]^{-1}$	$S^P_{44}\times 10^5$ $[\text{lbs}\cdot\text{in}^2]^{-1}$
1	2.665	2.666	11.25	11.21
2	1.884	1.899	6.445	6.297
3	2.018	2.098	6.836	6.674
4	2.380	2.376	8.332	8.336
5	5.620	5.622	6.120	6.130
6	10.60	10.35	5.903	5.915

Table 3: Extension-torsion and bending-torsion coupling components of the compliance matrix. Borri *et al.*: $(\cdot)^B$, present predictions: $(\cdot)^P$.

Lay-up	$S^B_{14}\times 10^6$ $[\text{lbs}\cdot\text{in}]^{-1}$	$S^P_{14}\times 10^6$ $[\text{lbs}\cdot\text{in}]^{-1}$	$S^B_{45}\times 10^5$ $[\text{lbs}\cdot\text{in}^2]^{-1}$	$S^P_{45}\times 10^5$ $[\text{lbs}\cdot\text{in}^2]^{-1}$
1	8.340	8.338	0	0
2	2.700	2.736	0	0
3	1.410	1.436	0	0
4	0	0	2.470	2.469
5	0	0	3.600	3.606
6	0	0	3.610	3.616

6.3 Curved beams

Figure 10 shows a curved beam with a uniform rectangular cross-section. The beam is made of homogenous, isotropic materials with Poisson's ratio $\nu = 0.3$. The dimensions of the cross-section are 1×0.01 and the beam's initial curvature is $k = 1/r = 1$; all data is presented in a non-dimensional form. Two loading cases are considered: *(a)* pure bending by a bending moment, M_3, and *(b)* bending by a tip shear force, Q. Since the thickness of the cross-section is far smaller than the height, plane stress state is assumed. For the two cases, analytical solutions can be obtained from elasticity theory [26]. In the present method, a 20×1 mesh of quadrilateral, nine-node elements is used for the cross-section.

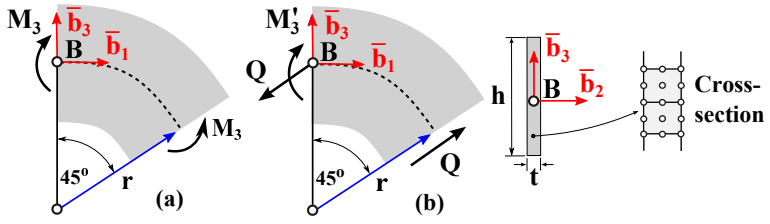

Figure 10: Curved planar beam.

For case *(a)*, the stress distribution over the cross-section is uniform along the beam's span. The non-dimensional axial and in-plane stresses distributions over the cross-section, denoted $th^2\sigma_{11}/6M_3$ and $th^2\sigma_{33}/6M_3$, respectively, are shown in figs. 11 and 12, respectively. For case *(b)*, the non-dimensional axial and in-plane stress distributions over the cross-section at the right-end of the beam, denoted $th\sigma_{11}/(3\sqrt{2}Q)$ and $th\sigma_{33}/(3\sqrt{2}Q)$, respectively, are depicted in figs. 13 and 14, respectively. For both loading cases, the proposed solutions are in excellent agreement with the analytical solutions.

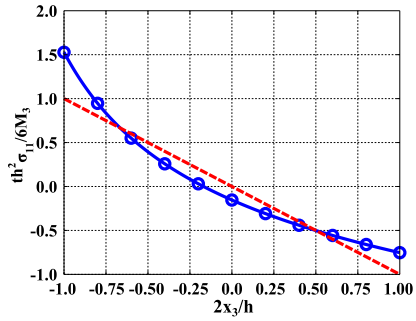

Figure 11: Distribution of the non-dimensional axial stress, σ_{11}. Analytical solution: solid line, present solution: ∘. For reference, the straight beam case is shown in the dashed line.

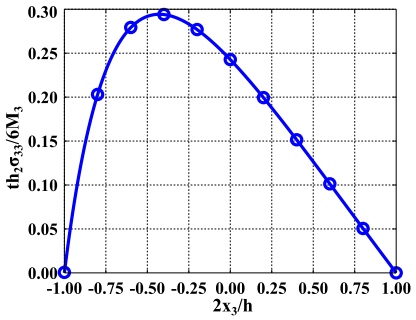

Figure 12: Distribution of the non-dimensional in-plane stress, σ_{33}. Analytical solution: solid line, present solution: ∘. For the straight beam, in-plane stress vanishes.

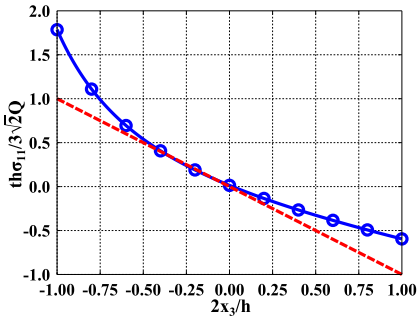

Figure 13: Distribution of the non-dimensional axial stress, σ_{11}. Analytical solution: solid line, present solution: ∘. For reference, the straight beam case is shown in the dashed line.

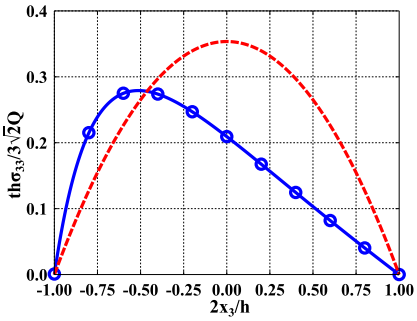

Figure 14: Distribution of the non-dimensional in-plane stress, σ_{33}. Analytical solution: solid line, present solution: ∘. For reference, the straight beam case is shown in the dashed line.

6.4 Cantilevered beam with a 45-degree bend

To illustrate the effects of initial curvature on the solution of beam problems, the response of the 45-degree bend cantilevered beam shown in figure 15 is investigated. The beam is cantilevered at point **O** and subjected to a concentrated tip load, P, acting along unit vector $\bar{\imath}_3$. The initial curvature of the beam about unit vector in $\bar{\imath}_3$ is k_3 = -0.01 in^{-1}. The cross-section of the beam is 2 × 2 in^2. The thin walls consist of six, 0.005 in thick plies of graphite/epoxy material with the following material properties: longitudinal modulus E_L = 20.59 Msi, transverse modulus E_T = 1.42 Msi, shearing modulus G_{LT} = 0.87 Msi, and Poisson's ratios ν_{LT} = 0.30, ν_{TN} = 0.34. The wall lay-ups are defined in fig. 15.

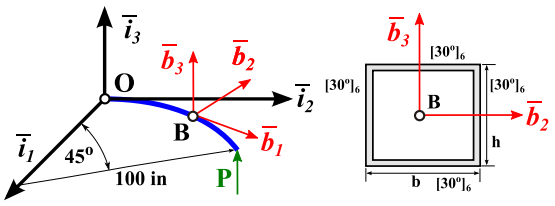

Figure 15: Cantilevered beam with a 45-degree bend.

Using a 40 × 6 mesh of nine-node, quadrilateral elements to discretize each wall, the proposed

approach yielded the beam's sectional stiffness matrix as

$$\underline{\underline{K}}_c^* = 10^6 \times \begin{bmatrix} 1.689 & 0.000 & 0.006 & -0.692 & 0.000 & 0.023 \\ -0.000 & 0.161 & 0.000 & 0.000 & 0.167 & 0.000 \\ 0.006 & 0.000 & 0.146 & -0.005 & 0.000 & 0.191 \\ -0.692 & 0.000 & -0.005 & 0.549 & 0.000 & -0.012 \\ -0.000 & 0.167 & 0.000 & 0.000 & 0.575 & 0.000 \\ 0.023 & 0.000 & 0.191 & -0.012 & 0.000 & 0.757 \end{bmatrix}.$$

For reference, the sectional stiffness matrix for a *straight* beam featuring the same cross-sectional configuration was obtained using the same mesh and setting $\kappa_3 = 0$,

$$\underline{\underline{K}}_s^* = 10^6 \times \begin{bmatrix} 1.816 & 0.000 & 0.000 & -0.744 & 0.000 & 0.000 \\ 0.000 & 0.240 & 0.000 & 0.000 & 0.378 & 0.000 \\ 0.000 & 0.000 & 0.240 & 0.000 & 0.000 & 0.378 \\ -0.744 & 0.000 & 0.000 & 0.571 & 0.000 & 0.000 \\ 0.000 & 0.378 & 0.0000 & 0.000 & 1.144 & 0.000 \\ 0.000 & 0.000 & 0.378 & 0.000 & 0.000 & 1.144 \end{bmatrix}.$$

Although the initial curvature is quite small (k_3 = -0.01 in^{-1}), matrices $\underline{\underline{K}}_c^*$ and $\underline{\underline{K}}_s^*$ differ significantly. Next, the deflections of the beam under tip loads $P_1 = 20$, $P_2 = 100$, and $P_3 = 200$ lbs are predicted. For each loading case, two different runs were performed, the first using $\underline{\underline{K}}_c^*$, the second using $\underline{\underline{K}}_s^*$.

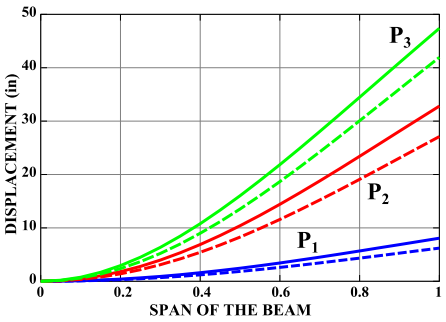

Figure 16: Displacement u_3, along unit vector $\bar{\imath}_3$ vs. beam span, for the three loading cases. Using $\underline{\underline{K}}_c^*$: solid line; using $\underline{\underline{K}}_s^*$: dashed line.

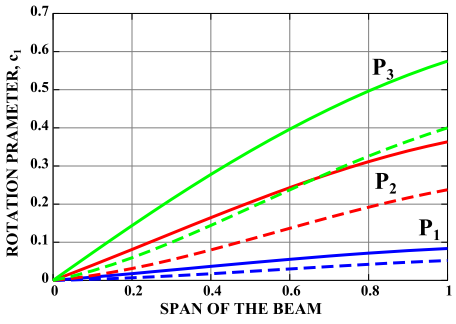

Figure 17: Rotation parameter c_1 about unit vector $\bar{\imath}_1$ vs. beam span, for the three loading cases. Using $\underline{\underline{K}}_c^*$: solid line; using $\underline{\underline{K}}_s^*$: dashed line.

Figures 16 and 17 show the displacement and rotation parameter, respectively, along the beam's span, for the three loading cases. Figures 18 and 19 depict the distributions of torque and bending moment along the beam span for the same loading cases. Large discrepancies are observed between the predictions obtained with the correct stiffness matrix for the curved beam, $\underline{\underline{K}}_c^*$, and those obtained from the stiffness matrix for the straight beam, $\underline{\underline{K}}_s^*$. This simple example illustrates the importance of evaluating the correct sectional stiffness matrix for beam problems. The methodology developed in this paper evaluates the correct stiffness matrix from three-dimensional elasticity.

7 Conclusions

This paper has presented a novel method for the analysis of beams based on the Hamiltonian formalism. The approach proceeds through a set of structure preserving transformations using symplectic matrices and decomposes the solution into its central and extremity components. The central solution is an exact solution of the linear theory of three-dimensional elasticity for beams

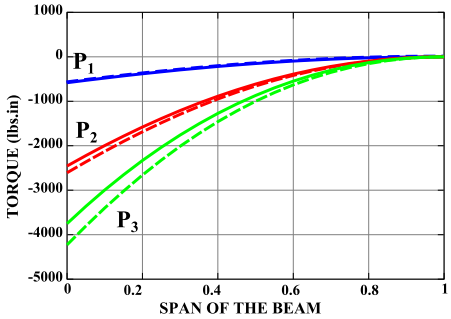

Figure 18: Torque M_1 about unit vector $\bar{b}_1$ vs. beam span, for the three loading cases. Using $\underline{\underline{K}}_c^*$: solid line; using $\underline{\underline{K}}_s^*$: dashed line.

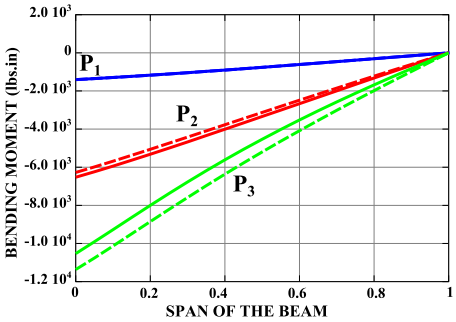

Figure 19: Bending moment M_2 about unit vector $\bar{b}_2$ vs. beam span, for the three loading cases. Using $\underline{\underline{K}}_c^*$: solid line; using $\underline{\underline{K}}_s^*$: dashed line.

presenting uniform geometric and material characteristics along their span and is valid far away from the beam's edges, where all extremity solutions become negligible. The kinematic assumptions underpinning commonly used beam theories have been eliminated altogether and yet, exact solutions are obtained for the central behavior of the beam.

This paper further generalizes the theory to naturally curved and twisted beams undergoing large motions. Kinematically, the problem is decomposed into a rigid-section motion and a warping field. The sectional strains associated with rigid-section motion and the warping field are assumed to remain small. As a natural consequence of this kinematic decomposition, the governing equations of the problem fall into two distinct categories: the equations describing geometrically exact beams and those describing local deformations. The average rigid-section motions of geometrically exact beams are governed by nonlinear, one-dimensional equations, whereas a linear, two-dimensional analysis provides the detailed distribution of three-dimensional stresses and strains. Given the stated assumptions, the solutions presented here are exact solution of three-dimensional elasticity for beams undergoing arbitrarily large motions, within the discretization error inherent to the finite element approach.

Numerical examples have been presented to demonstrate the capabilities of the analysis. The evaluation of the sectional stiffness matrix of a rectangular box-beam made of anisotropic materials was presented and the predictions were found to be in close agreement with results published in the literature. The detailed stress distributions in a homogeneous, curved beam were found to be in excellent agreement with elasticity solutions. Finally, the effect of initial curvature on the components of the sectional stiffness matrix and large deflection of a curved beam were illustrated.

A Hamiltonian matrices

Matrix $\underline{\underline{\bar{\mathcal{H}}}}$, of size $2n \times 2n$, is said to be Hamiltonian if it satisfies the following property

$$(\underline{\underline{\mathcal{J}}}\,\underline{\underline{\bar{\mathcal{H}}}})^T = \underline{\underline{\mathcal{J}}}\,\underline{\underline{\bar{\mathcal{H}}}}, \tag{73}$$

where skew-symmetric matrix $\underline{\underline{\mathcal{J}}}$ is defined as

$$\underline{\underline{\mathcal{J}}} = \begin{bmatrix} \underline{\underline{0}}_{n\times n} & \underline{\underline{I}}_{n\times n} \\ -\underline{\underline{I}}_{n\times n} & \underline{\underline{0}}_{n\times n} \end{bmatrix}. \tag{74}$$

Note the following properties of matrix $\underline{\underline{\mathcal{J}}}$,

$$\underline{\underline{\mathcal{J}}}^T = -\underline{\underline{\mathcal{J}}}, \tag{75a}$$

$$\underline{\underline{\mathcal{J}}}\,\underline{\underline{\mathcal{J}}}^T = \underline{\underline{\mathcal{I}}}. \tag{75b}$$

In view of these properties, the definition (73) of Hamiltonian matrices can be recast as $\underline{\underline{\bar{\mathcal{H}}}} = \underline{\underline{\mathcal{J}}}\,\underline{\underline{\bar{\mathcal{H}}}}^T\,\underline{\underline{\mathcal{J}}}$. Because matrix $\underline{\underline{\mathcal{J}}}$ is skew-symmetric, the following property holds for any vector $\underline{\mathcal{U}}$,

$$\underline{\mathcal{U}}^T\,\underline{\underline{\mathcal{J}}}\,\underline{\mathcal{U}} = 0. \tag{76}$$

Property (73) implies that the most general form of a Hamiltonian matrix is

$$\underline{\underline{\bar{\mathcal{H}}}} = \begin{bmatrix} \underline{\underline{A}} & \underline{\underline{B}} \\ \underline{\underline{C}} & -\underline{\underline{A}}^T \end{bmatrix}, \tag{77}$$

where matrices $\underline{\underline{A}}$, $\underline{\underline{B}}$, and $\underline{\underline{C}}$ are of size $n \times n$, and matrices $\underline{\underline{B}}$ and $\underline{\underline{C}}$ are symmetric. Clearly, the transpose of a Hamiltonian matrix is also Hamiltonian.

A.1 Eigenvalues of Hamiltonian matrices

Let λ and μ be two eigenvalues of a Hamiltonian matrix and the associated eigenvectors are denoted $\underline{\mathcal{U}}_\lambda$ and $\underline{\mathcal{U}}_\mu$, respectively, *i.e.*, $\underline{\underline{\bar{\mathcal{H}}}}\,\underline{\mathcal{U}}_\lambda = \lambda\underline{\mathcal{U}}_\lambda$ and $\underline{\underline{\bar{\mathcal{H}}}}\,\underline{\mathcal{U}}_\mu = \mu\underline{\mathcal{U}}_\mu$. Pre-multiplying the first equation by $\underline{\mathcal{U}}_\mu^T\underline{\underline{\mathcal{J}}}$ and the second by $\underline{\mathcal{U}}_\lambda^T\underline{\underline{\mathcal{J}}}$ leads to $\underline{\mathcal{U}}_\mu^T\underline{\underline{\mathcal{J}}}\,\underline{\underline{\bar{\mathcal{H}}}}\,\underline{\mathcal{U}}_\lambda = \lambda\underline{\mathcal{U}}_\mu^T\underline{\underline{\mathcal{J}}}\,\underline{\mathcal{U}}_\lambda$ and $\underline{\mathcal{U}}_\lambda^T\underline{\underline{\mathcal{J}}}\,\underline{\underline{\bar{\mathcal{H}}}}\,\underline{\mathcal{U}}_\mu = \mu\underline{\mathcal{U}}_\lambda^T\underline{\underline{\mathcal{J}}}\,\underline{\mathcal{U}}_\mu$, respectively. Because matrix $\underline{\underline{\mathcal{J}}}\,\underline{\underline{\bar{\mathcal{H}}}}$ is symmetric, the right-hand sides of these two equations are identical and subtraction yields $(\lambda+\mu)\underline{\mathcal{U}}_\mu^T\underline{\underline{\mathcal{J}}}\,\underline{\mathcal{U}}_\lambda = 0$. If $\lambda + \mu \neq 0$, the following symplectic orthogonality results,

$$\underline{\mathcal{U}}_\mu^T\underline{\underline{\mathcal{J}}}\,\underline{\mathcal{U}}_\lambda = 0. \tag{78}$$

Let λ be an eigenvalue of a Hamiltonian matrix associated with eigenvector $\underline{\mathcal{U}}_{+\lambda}$, *i.e.*, $\underline{\underline{\bar{\mathcal{H}}}}\,\underline{\mathcal{U}}_{+\lambda} = \lambda\underline{\mathcal{U}}_{+\lambda}$. It then follows that $\underline{\underline{\mathcal{J}}}\,\underline{\underline{\bar{\mathcal{H}}}}\,\underline{\mathcal{U}}_{+\lambda} = \lambda\underline{\underline{\mathcal{J}}}\,\underline{\mathcal{U}}_{+\lambda}$ and properties (73) and (75a) then imply $\underline{\underline{\bar{\mathcal{H}}}}^T(\underline{\underline{\mathcal{J}}}\,\underline{\mathcal{U}}_{+\lambda}) = -\lambda(\underline{\underline{\mathcal{J}}}\,\underline{\mathcal{U}}_{+\lambda})$. Clearly, if $\underline{\mathcal{U}}_{+\lambda}$ is an eigenvector of $\underline{\underline{\bar{\mathcal{H}}}}$ associated with eigenvalue λ, $\underline{\underline{\mathcal{J}}}\,\underline{\mathcal{U}}_{+\lambda}$ is an eigenvector of $\underline{\underline{\bar{\mathcal{H}}}}^T$ associated with eigenvalue $-\lambda$. Because the spectra of eigenvalues of matrices $\underline{\underline{\bar{\mathcal{H}}}}$ and $\underline{\underline{\bar{\mathcal{H}}}}^T$ are identical, the eigenvalues of Hamiltonian matrices are symmetric about the imaginary axis, *i.e.*, occur in pairs of opposite sign, $\pm\lambda$. In summary,

$$\left(\underline{\underline{\bar{\mathcal{H}}}} - \lambda\underline{\underline{\mathcal{I}}}\right)\underline{\mathcal{U}}_{+\lambda} = \underline{0} \Longleftrightarrow \left(\underline{\underline{\bar{\mathcal{H}}}}^T + \lambda\underline{\underline{I}}\right)(\underline{\underline{\mathcal{J}}}\,\underline{\mathcal{U}}_{+\lambda}) = \underline{0}, \tag{79a}$$

$$\left(\underline{\underline{\bar{\mathcal{H}}}} + \lambda\underline{\underline{\mathcal{I}}}\right)\underline{\mathcal{U}}_{-\lambda} = \underline{0} \Longleftrightarrow \left(\underline{\underline{\bar{\mathcal{H}}}}^T - \lambda\underline{\underline{I}}\right)(\underline{\underline{\mathcal{J}}}\,\underline{\mathcal{U}}_{-\lambda}) = \underline{0}, \tag{79b}$$

where eqs (79a) and (79b) express identical properties for eigenvalues $+\lambda$ and $-\lambda$, respectively. Vectors $\underline{\mathcal{U}}_{+\lambda}$ and $\underline{\underline{\mathcal{J}}}\,\underline{\mathcal{U}}_{-\lambda}$ can also be interpreted as the right and left eigenvectors of matrix $\underline{\underline{\bar{\mathcal{H}}}}$ both associated with eigenvalue $+\lambda$.

It is convenient to define matrix $\underline{\underline{\mathcal{U}}}_{\mp\lambda} = \left[\underline{\mathcal{U}}_{-\lambda}, \underline{\mathcal{U}}_{+\lambda}\right]$, whose columns store the right eigenvectors associated with eigenvalues $-\lambda$ and $+\lambda$. These vectors enjoy the following properties

$$\underline{\underline{\mathcal{U}}}_{\mp\lambda}^T\underline{\underline{\mathcal{J}}}\,\underline{\underline{\mathcal{U}}}_{\mp\lambda} = \begin{bmatrix} 0 & 1 \\ -1 & 0 \end{bmatrix}. \tag{80}$$

Indeed, property (76) implies $\underline{\mathcal{U}}_{+\lambda}^T\underline{\underline{\mathcal{J}}}\,\underline{\mathcal{U}}_{+\lambda} = \underline{\mathcal{U}}_{-\lambda}^T\underline{\underline{\mathcal{J}}}\,\underline{\mathcal{U}}_{-\lambda} = 0$ and vectors $\underline{\mathcal{U}}_{+\lambda}$ and $\underline{\mathcal{U}}_{-\lambda}$ can be normalized to enforce $\underline{\mathcal{U}}_{-\lambda}^T\underline{\underline{\mathcal{J}}}\,\underline{\mathcal{U}}_{+\lambda} = 1$. The following pseudo-orthogonality statement in the space of Hamiltonian matrix then follows

$$\underline{\underline{\mathcal{U}}}_{\mp\lambda}^T\underline{\underline{\mathcal{J}}}\,\underline{\underline{\bar{\mathcal{H}}}}\,\underline{\underline{\mathcal{U}}}_{\mp\lambda} = \begin{bmatrix} 0 & \lambda \\ \lambda & 0 \end{bmatrix}. \tag{81}$$

B Symplectic matrices

Matrix $\underline{\underline{\mathcal{S}}}$, of size $2n \times 2n$, is said to be symplectic if it satisfies the following property

$$\underline{\underline{\mathcal{S}}}^T \underline{\underline{\mathcal{J}}} \underline{\underline{\mathcal{S}}} = \underline{\underline{\mathcal{J}}}, \tag{82}$$

where skew-symmetric matrix $\underline{\underline{\mathcal{J}}}$ is defined by eq. (74). The inverse of a symplectic matrix is expressed easily as

$$\underline{\underline{\mathcal{S}}}^{-1} = \underline{\underline{\mathcal{J}}}^T \underline{\underline{\mathcal{S}}}^T \underline{\underline{\mathcal{J}}}. \tag{83}$$

Indeed, using definition (82) leads to $\underline{\underline{\mathcal{S}}}^{-1}\underline{\underline{\mathcal{S}}} = \underline{\underline{\mathcal{J}}}^T \underline{\underline{\mathcal{S}}}^T \underline{\underline{\mathcal{J}}}\,\underline{\underline{\mathcal{S}}} = \underline{\underline{\mathcal{J}}}^T \underline{\underline{\mathcal{J}}} = \underline{\underline{\mathcal{I}}}$.

Recasting eq. (82) as $\underline{\underline{\mathcal{J}}} = \underline{\underline{\mathcal{S}}}^{-T} \underline{\underline{\mathcal{J}}}\, \underline{\underline{\mathcal{S}}}^{-1}$ and using eq. (83) to express the inverse of the symplectic matrix leads to $\underline{\underline{\mathcal{J}}} = (\underline{\underline{\mathcal{J}}}^T \underline{\underline{\mathcal{S}}}^T \underline{\underline{\mathcal{J}}})^T \underline{\underline{\mathcal{J}}} (\underline{\underline{\mathcal{J}}}^T \underline{\underline{\mathcal{S}}}^T \underline{\underline{\mathcal{J}}})$, and finally

$$\underline{\underline{\mathcal{S}}} \underline{\underline{\mathcal{J}}} \underline{\underline{\mathcal{S}}}^T = \underline{\underline{\mathcal{J}}}. \tag{84}$$

This means that the transpose of a symplectic matrix is itself symplectic. It is proved easily that if matrix $\underline{\underline{\mathcal{S}}}$ is symplectic, its inverse is also symplectic. Furthermore, the product of two symplectic matrices is also symplectic. Note that matrices $\underline{\underline{\mathcal{J}}}$ and $\underline{\underline{\mathcal{I}}}$ are symplectic.

A close connection exists between symplectic and Hamiltonian matrices. First, their definitions are closely related: $\underline{\underline{\bar{\mathcal{H}}}} = \underline{\underline{\mathcal{J}}}\, \underline{\underline{\bar{\mathcal{H}}}}^T \underline{\underline{\mathcal{J}}}$ and $\underline{\underline{\mathcal{S}}}^T \underline{\underline{\mathcal{J}}} \underline{\underline{\mathcal{S}}} = \underline{\underline{\mathcal{J}}}$, for Hamiltonian and symplectic matrices, respectively. Next, consider matrix $\underline{\underline{\hat{\mathcal{H}}}}$, defined through the following transformation, $\underline{\underline{\hat{\mathcal{H}}}} = \underline{\underline{\mathcal{S}}}^{-1} \underline{\underline{\bar{\mathcal{H}}}}\, \underline{\underline{\mathcal{S}}}$. Using eq. (83) leads to $\underline{\underline{\mathcal{J}}}\, \underline{\underline{\hat{\mathcal{H}}}} = \underline{\underline{\mathcal{J}}} (\underline{\underline{\mathcal{J}}}^T \underline{\underline{\mathcal{S}}}^T \underline{\underline{\mathcal{J}}}) \underline{\underline{\bar{\mathcal{H}}}}\, \underline{\underline{\mathcal{S}}} = \underline{\underline{\mathcal{S}}}^T (\underline{\underline{\mathcal{J}}}\, \underline{\underline{\bar{\mathcal{H}}}}) \underline{\underline{\mathcal{S}}}$, which implies that matrix $\underline{\underline{\mathcal{J}}}\, \underline{\underline{\hat{\mathcal{H}}}}$ is symmetric if matrix $(\underline{\underline{\mathcal{J}}}\, \underline{\underline{\bar{\mathcal{H}}}})$ is itself symmetric. Consequently, if matrix $\underline{\underline{\bar{\mathcal{H}}}}$ is Hamiltonian, so is matrix $\underline{\underline{\hat{\mathcal{H}}}}$. It follows that the transformation of a Hamiltonian matrix by a symplectic matrix yields a Hamiltonian matrix, *i.e.*,

$$\underline{\underline{\hat{\mathcal{H}}}} = \underline{\underline{\mathcal{S}}}^{-1} \underline{\underline{\bar{\mathcal{H}}}}\, \underline{\underline{\mathcal{S}}}. \tag{85}$$

Consider the following partition of a symplectic matrix

$$\underline{\underline{\mathcal{S}}} = \begin{bmatrix} \underline{\underline{A}} & \underline{\underline{B}} \\ \underline{\underline{C}} & \underline{\underline{D}} \end{bmatrix}, \tag{86}$$

where matrices $\underline{\underline{A}}$, $\underline{\underline{B}}$, $\underline{\underline{C}}$, and $\underline{\underline{D}}$ are of size $n \times n$. The definition of a symplectic matrix then implies

$$\underline{\underline{A}}^T \underline{\underline{D}} - \underline{\underline{C}}^T \underline{\underline{B}} = \underline{\underline{I}}, \tag{87a}$$

$$\left(\underline{\underline{A}}^T \underline{\underline{C}}\right) = \left(\underline{\underline{A}}^T \underline{\underline{C}}\right)^T, \tag{87b}$$

$$\left(\underline{\underline{B}}^T \underline{\underline{D}}\right) = \left(\underline{\underline{B}}^T \underline{\underline{D}}\right)^T. \tag{87c}$$

The last two properties imply that products $\underline{\underline{A}}^T \underline{\underline{C}}$ and $\underline{\underline{B}}^T \underline{\underline{D}}$ form symmetric matrices.

References

[1] O.A. Bauchau and J.I. Craig. *Structural Analysis with Application to Aerospace Structures*. Springer, Dordrecht, Heidelberg, London, New-York, 2009.

[2] V. Giavotto, M. Borri, P. Mantegazza, G. Ghiringhelli, V. Carmaschi, G.C. Maffioli, and F. Mussi. Anisotropic beam theory and applications. *Computers & Structures*, 16(1-4):403–413, 1983.

[3] A. Mielke. Saint-Venant's problem and semi-inverse solutions in nonlinear elasticity. *Archive of Rational Mechanics and Analysis*, 102:205–229, 1988.

[4] A. Mielke. Normal hyperbolicity of center manifolds and Saint-Venant's principle. *Archive of Rational Mechanics and Analysis*, 110:353–372, December 1990.

[5] A. Mielke. *Hamiltonian and Lagrangian Flows on Center Manifolds with Applications to Elliptic Variational Problems*. Springer, Berlin, Heidelberg, 1991. Lecture Notes in Mathematics, Vol. 1489.

[6] W.X. Zhong. *A New Systematic Methodology for Theory of Elasticity*. Dalian University of Technology Press, Dalian, 1995.

[7] W.X. Zhong, X.S. Xu, and H.W. Zhang. Hamiltonian system and the Saint-Venant problem in elasticity. *Applied Mathematics and Mechanics*, 17(9):827–836, 1996.

[8] W.A. Yao, W.X. Zhong, and C.W. Lim. *Symplectic Elasticity*. World Scientific Publishing Co. Pte. Ltd., New Jersey, 2009.

[9] M. Morandini, M. Chierichetti, and P. Mantegazza. Characteristic behavior of prismatic anisotropic beam via generalized eigenvectors. *International Journal of Solids and Structures*, 47:1327–1337, 2010.

[10] V.L. Berdichevsky. On the energy of an elastic rod. *Prikladnaya Matematika y Mekanika*, 45(4):518–529, 1982.

[11] D.H. Hodges. A review of composite rotor blade modeling. *AIAA Journal*, 28(3):561–565, March 1990.

[12] O.A. Bauchau and S.L. Han. Three-dimensional beam theory for flexible multibody dynamics. *Journal of Computational and Nonlinear Dynamics*, 9(4):041011 (12 pages), 2014.

[13] J.C. Simo and L. Vu-Quoc. On the dynamics in space of rods undergoing large motions - A geometrically exact approach. *Computer Methods in Applied Mechanics and Engineering*, 66(1):125–161, 1988.

[14] M. Borri and T. Merlini. A large displacement formulation for anisotropic beam analysis. *Meccanica*, 21:30–37, 1986.

[15] D.A. Danielson and D.H. Hodges. A beam theory for large global rotation, moderate local rotation, and small strain. *Journal of Applied Mechanics*, 55(1):179–184, 1988.

[16] O.A. Bauchau. *Flexible Multibody Dynamics*. Springer, Dordrecht, Heidelberg, London, New-York, 2011.

[17] V.V. Volovoi, D.H. Hodges, V.L. Berdichevsky, and V.G. Sutyrin. Dynamic dispersion curves for non-homogeneous, anisotropic beams with cross sections of arbitrary geometry. *Journal of Sound and Vibration*, 215:1101–1120, 1998.

[18] C. Lanczos. *The Variational Principles of Mechanics*. Dover Publications, Inc., New York, 1970.

[19] J. C.-B. de Saint-Venant. Mémoire sur la torsion des prismes. *Receuil des Savants Étrangers*, 14:233–560, 1855.

[20] J.C. Simo. A finite strain beam formulation. The three-dimensional dynamic problem. Part I. *Computer Methods in Applied Mechanics and Engineering*, 49(1):55–70, 1985.

[21] J.C. Simo and L. Vu-Quoc. A three-dimensional finite strain rod model. Part II: Computational aspects. *Computer Methods in Applied Mechanics and Engineering*, 58(1):79–116, 1986.

[22] D.A. Danielson and D.H. Hodges. Nonlinear beam kinematics by decomposition of the rotation tensor. *Journal of Applied Mechanics*, 54(2):258–262, 1987.

[23] A.R. Atilgan and D.H. Hodges. Unified nonlinear analysis for nonhomogeneous anisotropic beams with closed cross-sections. *AIAA Journal*, 29(11):1990–1999, November 1991.

[24] A.R. Atilgan, D.H. Hodges, and M.V. Fulton. Nonlinear deformation of composite beams: Unification of cross-sectional and elastica analyses. *Applied Mechanics Reviews*, 44(11):S9–S15, November 1991.

[25] M. Borri, G.L. Ghiringhelli, and T. Merlini. Linear analysis of naturally curved and twisted anisotropic beams. *Composites Engineering*, 2(5-7):433–456, 1992.

[26] S.P. Timoshenko and J.N. Goodier. *Theory of Elasticity*. McGraw-Hill Book Company, New York, third edition, 1970.